AFCEC-CX-TY-TR-2013-0001

EFFECT OF WATER ABSORPTION AND OUTDOOR WEATHERING ON EMERGING POLYMER INTERLAYERS: A THESIS PRESENTED TO THE FACULTY OF THE GRADUATE SCHOOL OF THE UNIVERSITY OF MISSOURI – COLUMBIA

Brooke Marie Dean
University of Missouri
115 Business Loop 70 West
Mizzou, North 501
Columbia, MO 65211

Battelle Memorial Institute
505 King Ave
Columbus, Ohio 43201-2696

Contract Number: FA8051-19-F-A020

April 2021

AIR FORCE CIVIL ENGINEER CENTER
READINESS DIRECTORATE

■ **Requirements & Acquisition Division** ■ **United States Air Force** ■ **Tyndall Air Force Base, FL 32403-5323**

DISCLAIMER

Reference herein to any specific commercial product, process, or service by trade name, trademark, manufacturer, or otherwise does not constitute or imply its endorsement, recommendation, or approval by the United States Air Force. The views and opinions of authors expressed herein do not necessarily state or reflect those of the United States Air Force.

This report was prepared as an account of work sponsored by the United States Air Force. Neither the United States Air Force, nor any of its employees, makes any warranty, expressed or implied, or assumes any legal liability or responsibility for the accuracy, completeness, or usefulness of any information, apparatus, product, or process disclosed, or represents that its use would not infringe privately owned rights.

REPORT DOCUMENTATION PAGE

Form Approved
OMB No. 0704-0188

PLEASE DO NOT RETURN YOUR FORM TO THE ABOVE ADDRESS.

1. REPORT DATE *(DD-MM-YYYY)*	2. REPORT TYPE	3. DATES COVERED *(From - To)*
01-04-2021	Master's Thesis	Jan 2020 to Apr 2021

4. TITLE AND SUBTITLE

Effect of Water Absorption and Outdoor Weathering on Emerging Polymer Interlayers: A Thesis Presented to the Faculty of the Graduate School of the University of Missouri – Columbia

5a. CONTRACT NUMBER

FA8051-19-F-A020

5b. GRANT NUMBER

5c. PROGRAM ELEMENT NUMBER

6. AUTHOR(S)

Brooke Marie Dean

5d. PROJECT NUMBER

5e. TASK NUMBER

5f. WORK UNIT NUMBER

7. PERFORMING ORGANIZATION NAME(S) AND ADDRESS(ES)

University of Missouri
115 Business Loop 70 West
Mizzou, North 501
Columbia, MO 65211

8. PERFORMING ORGANIZATION REPORT NUMBER

9. SPONSORING/MONITORING AGENCY NAME(S) AND ADDRESS(ES)

U.S. Air Force, AFCEC/CXAE
Airbase Technologies Branch
139 Barnes Dr. Suite 2
Tyndall, AFB, FL 32403

10. SPONSOR/MONITOR'S ACRONYM(S)

11. SPONSOR/MONITOR'S REPORT NUMBER(S)

AFCEC-CX-TY-TR-2021-0018

12. DISTRIBUTION/AVAILABILITY STATEMENT

DISTRIBUTION A. Approved for public release. Distribution Unlimited. AFCEC-20211110; 7 May 2021

13. SUPPLEMENTARY NOTES

14. ABSTRACT

Laminated glass windows are becoming increasingly popular in the structures industry. Because of this, new polymer interlayer materials are being developed to better serve the purposes of building design, rather than windshield design, which was the original purpose. Since buildings are designed to stand the test of time, it is important to understand how the laminated glass windows, and in turn the polymer interlayer materials, will behave after weathering action. It is known that weathering action has a significant impact on polymer interlayer materials, and previous studies have evaluated certain aspects of weathering such as temperature, humidity, and UV radiation. The purpose of this research is to gain a better understanding of the difference in impact of weathering on various emerging polymer interlayer materials. This study will take a brief look at the effects of strain rate on the mechanical behavior of polymer interlayers before focusing on the effects of water absorption and outdoor weathering on PVB, EVA, and SG. The mechanical behavior will be evaluated using quasi-static and high strain rate testing after exposure to weathering conditions. In addition, the difference in natural aging of polymers between two glass plies will be compared to those with direct exposure to investigate the impact of the glass on the weathering affects. The research presented herein is ongoing, and the full scope of the project will be discussed as future work.

15. SUBJECT TERMS

Window, Laminated Glass, Polyvinyl butyral (PVB), SentryGlass (SG), Ethylene-vinyl acetate (EVA)

16. SECURITY CLASSIFICATION OF:			17. LIMITATION OF ABSTRACT	18. NUMBER OF PAGES	19a. NAME OF RESPONSIBLE PERSON
a. REPORT	b. ABSTRACT	c. THIS PAGE			Kevin Wise
U	U	U	SAR	95	19b. TELEPHONE NUMBER *(Include area code)* 850-283-6099

Effect of Water Absorption and Outdoor Weathering on Emerging Polymer Interlayers

A Thesis Presented to the Faculty of the Graduate School of the

University of Missouri – Columbia

In Partial Fulfillment of the Requirements for the Degree

Master of Science In

Civil and Environmental Engineering

By

Brooke Marie Dean

Dr. Hani Salim, Thesis Supervisor

APRIL 2021

The undersigned, appointed by the dean of the Graduate School, have examined the thesis entitled

"Effect of Water Absorption and Outdoor Weathering on Emerging Polymer Interlayers"

presented by Brooke Marie Dean,

a candidate for the degree of Master of Science in Civil and Environmental Engineering, and hereby certify that, in their opinion, it is worthy of acceptance.

Professor Hani Salim

Professor John Gahl

Professor Alaaeldin Elsisi

Acknowledgements

I would like to thank my committee chair and faculty advisor, Professor Hani Salim, for his encouragement and wisdom throughout my time in graduate school, and during the writing of this thesis.

I would like to thank the members of the research team, Dr. Aaron Saucier and Caleb Phillips, for their guidance in the research facility. I also want to express my appreciation for my fellow graduate student, Jon Knight, who led me through the process and generously offered his time and talents to help me succeed.

I would like to offer my sincere appreciation for my thesis committee, Dr. Alaaeldin Elsisi and Dr. John Gahl, for their time, comments, and continued interest in this research. I would also like to thank Dr. Elsisi for his assistance in static testing, data analysis, and literature review, and for developing the PhotoTrack software, which greatly simplified data analysis process.

Finally, I would like to thank Battelle Memorial Institute for providing financial support and valued collaboration with the Air Force Civil Engineer Center (AFCEC) at Tyndall Air Force Base and the United States Department of State.

TABLE OF CONTENTS

List of Figures

List of Tables

Abstract

Laminated glass windows are becoming increasingly popular in the structures industry. Because of this, new polymer interlayer materials are being developed to better serve the purposes of building design, rather than windshield design, which was the original purpose. Since buildings are designed to stand the test of time, it is important to understand how the laminated glass windows, and in turn the polymer interlayer materials, will behave after weathering action. It is known that weathering action has a significant impact on polymer interlayer materials, and previous studies have evaluated certain aspects of weathering such as temperature, humidity, and UV radiation. The purpose of this research is to gain a better understanding of the difference in impact of weathering on various emerging polymer interlayer materials. This study will take a brief look at the effects of strain rate on the mechanical behavior of polymer interlayers before focusing on the effects of water absorption and outdoor weathering on PVB, EVA, and SG. The mechanical behavior will be evaluated using quasi-static and high strain rate testing after exposure to weathering conditions. In addition, the difference in natural aging of polymers between two glass plies will be compared to those with direct exposure to investigate the impact of the glass on the weathering affects. The research presented herein is ongoing, and the full scope of the project will be discussed as future work.

1 INTRODUCTION

1.1 BACKGROUND

When an explosion occurs in the proximity of a building, it sends a pressure wave crashing into the exterior. The forces experienced by the members are unlike the typical forces accounted for in structural design because they require high energy absorption in a short period of time. The initial pressure wave causes damage to exterior and shatters windows. Without the windows, the pressure is able to enter the building and cause harm to its occupants. Injury can occur from hearing damage, or flying debris, including glass shards ("ISC Security Design Criteria", 2003). Since safety is the number one priority in engineering, it is important to investigate solutions that can mitigate the injuries of building occupants during a blast.

Laminated glass can help prevent the catastrophic failure of windows during a blast event. Laminated glass has a polymer interlayer between two or more glass panes. The interlayer is typically Polyvinyl butyral (PVB), but newer polymers including Ethylene-vinyl acetate (EVA), and SentryGlas® (SG) have been developed for this application in recent years. When a blast occurs and the glass cracks, the polymer interlayer is responsible for absorbing the energy and preventing the pressure wave from entering the building.

It is known that polymer interlayers are sensitive to weathering action, and the exposure of laminated glass interlayer to weathering factors, such as solar radiation, thermal cycles, or humidity, may affect the mechanical and optical properties of the polymeric interlayers, as well as its adhesion with glass (Ranocchiai et al., 2016). Ageing factors and their effect on

strength and durability are especially important for bond and adhesion. Bedon (2019) identified that degradation in the bonding region between the interlayer and glass could severely affect the structural performance of laminated glass, which includes the performance of the LG windows under extreme loads such as blast. Weathering is an important impact to consider when evaluating the mechanical behavior of polymer interlayers.

1.2 OBJECTIVES

The goal of this research is to experimentally evaluate the effect of strain-rate, water absorption and outdoor weathering on the mechanical characteristics of laminated glass interlayers. The results of this research are expected to enhance understanding of effect the environmental conditions on the long-term design of the LG windows against static and dynamic loads.

To achieve the objective of this project, the following tasks are realized:

- Collect and summarize relevant literature in area of environmental behavior and mechanical evaluation of laminated glass systems and interlayer polymers.
- Develop a methodology to apply and test the environmental effects on polymer interlayer. Environmental effects will include the outdoor weathering and water immersion.
- Experimentally evaluate PVB, EVA, and SG under high strain rates and quasi-static loading with and without aging and environmental effects.

1.3 SCOPE AND ORGANIZATION

This study focuses on the water absorption characteristics for three polymer interlayers: Polyvinyl butyral (PVB), Ethylene-vinyl acetate (EVA), and SentryGlas® (SG). The results of this study can be used to further understand the benefits and drawbacks of newly developed polymer interlayers compared to the current standard. The study will be organized as follows:

- Chapter 1 includes the background, objectives, and scope and organization.
- Chapter 2 reviews existing literature related to tensile testing, aging, natural weathering, and water absorption of polymers, describes the problem statement, and determines the need for further research in this area.
- Chapter 3 characterizes the strain-rate dependent behavior of each polymer interlayer.
- Chapter 4 presents and discusses the results of the outdoor weathering and water absorption studies. Results will be compared to a control group in which unconditioned specimens were tested at room temperature (68°F) and average relative humidity.
- Chapter 5 states the main conclusion, gives recommendations, and describes future work to continue this research.

2 LITERATURE REVIEW

2.1 INTRODUCTION

This section looks at existing literature related to laminated glass, polymer interlayer materials, tensile testing, and environmental effects. Through this review of existing literature, a hole was identified in the direct comparison of the environmental effects on original materials, such as PVB, and emerging materials such as EVA and SG. This study, as part of an ongoing project, will investigate and draw conclusions on the effects of water absorption and outdoor weathering on the mechanical behavior of PVB, EVA, and SG. The ultimate goal of the overarching research is to evaluate the individual and combined effects of temperature, humidity, and UV radiation on emerging polymer interlayers.

2.2 LAMINATED GLASS AND POLYMER INTERLAYER MATERIALS

Laminated glass (LG) consists of one or multiple polymer interlayer such as polyvinyl butyral (PVB), ethylene-vinyl acetate (EVA), or SentryGlas® (SG) bonding two or more glass layers together (Figure 1).

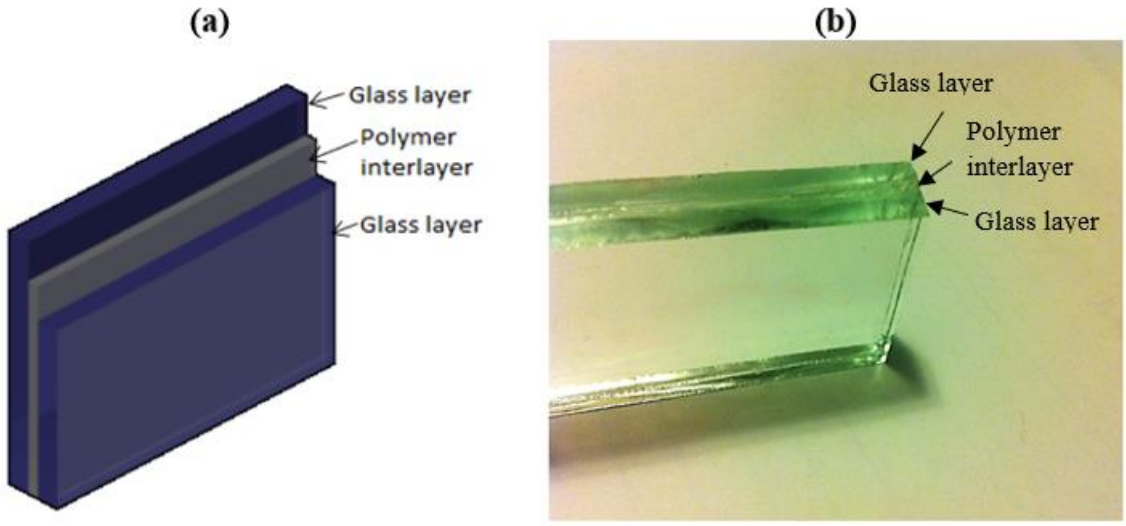

Figure 1: Laminated glass (a) schematic, (b) test specimen.

The glass layers can consist of annealed, heat strengthened, fully tempered, or a combination of glazing types. The bond occurs due to the chemical union between the hydroxyl groups of the polymer interlayer and the silanol groups of the glass layers (Martín et al., 2020). Production of laminated glass occurs by one of two methods: heat and pressure, or UV curing. In the heat and pressure method, an interlayer is placed between two glass sheets and air is removed. An autoclave or similar mechanism applies high pressures at the same time as high temperature is applied. Bonding is conducted at temperatures ranging from about 110°C to 140°C (Teotia & Soni, 2014). Residual stresses from heat bonding are retained. In the UV curing method, liquid interlayer resin is pumped into the cavity between the glass sheets and is later cured at ambient temperature by exposure to UV radiation. This method is far more cost effective and easier to perform than the heat a pressure method.

Laminated glass was first patented for use in car windshields. The interlayer polyvinyl butyral (PVB) was invented by Howard W. Matheson and Frederick W. Skirrow in 1927, which spurred the widespread use of the material in the automobile industry. This “safety glass”, as it was called, did not easily discolor with age nor shatter during accidents, thus making it a much better alternative than previously manufactured windshields.

Today, laminated glass is still used in car windshields, but has numerous uses outside the automobile industry including bullet proofing and structural applications. In building structures, LG windows are useful for extreme events such as hurricanes, earthquakes, and blasts. The laminated glass is able to absorb energy after cracking because of the properties of the polymer interlayer. This can prevent a pressure wave or strong wind from entering the building, thus preventing flying debris from harming those inside. The interlayer is also responsible for containing the glass shards should the window fail.

2.3 STRAIN RATE EFFECTS

Strain rate is defined in mechanics of materials as a rate of change in strain with respect to time and is denoted using the symbol ($\dot{\varepsilon}$). In tensile testing, tests are defined based on the order of magnitude of the strain rate (Figure 2). Quasi-static tensile tests are in the range 10^{-5} to 10^{-1} s^{-1} and are performed using servo-hydraulic machines which control the rate of displacement of two grips. High strain rate tests are in the range 10 and 10^{4} s^{-1}. High strain rates can be achieved using the Split-Hopkinson Bar testing technique or, more recently, servo-hydraulic machines are able to achieve high strain rates up to about 1000 s^{-1} (Chen et al., 2018). Polymer interlayers can be described as viscoelastic, meaning they are highly

strain rate dependent. Thus, it is important to ensure the desired strain rate is achieved when comparing results. Chapter 3 will further investigate the strain-rate dependence of PVB, EVA, and SG.

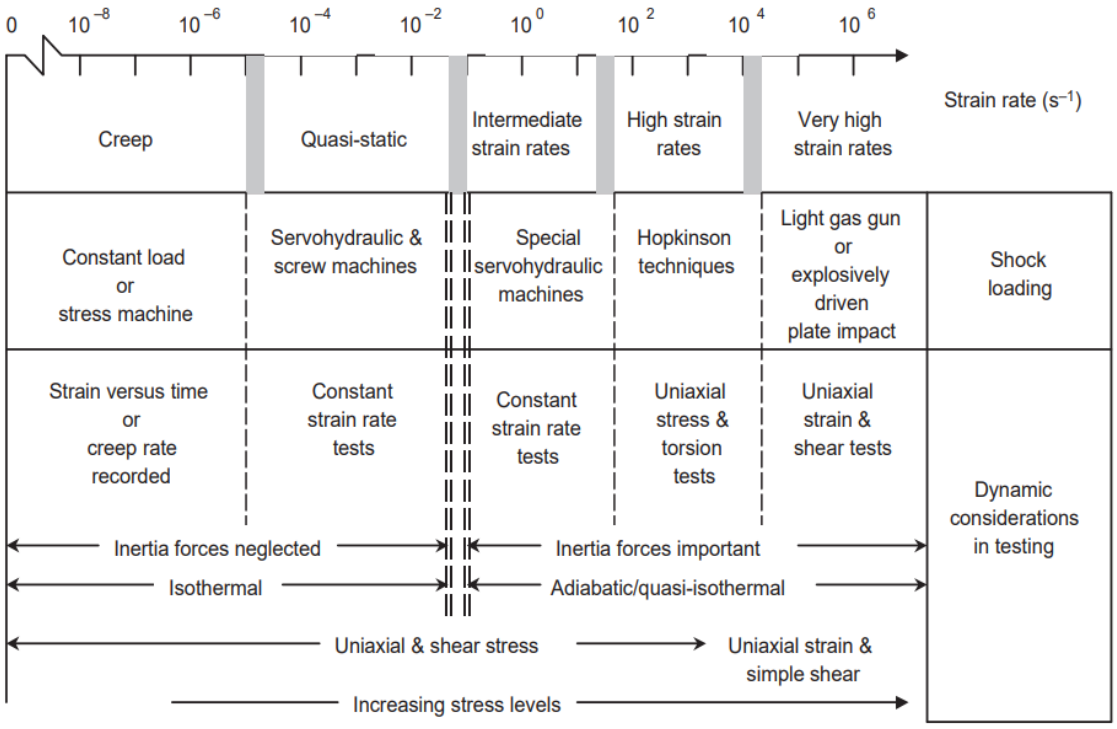

Figure 2: Strain rate regimes and associated instruments and experimental conditions (Nemat-Nasser, 2000).

2.4 ENVIRONMENTAL EFFECTS

Weathering action has a significant impact on the mechanical properties of polymer interlayers and can modify their behavior as a consequence of temperature, humidity, and solar radiation. Many studies demonstrate the significant influence of weathering on the physical and mechanical properties of PVB, the most commonly used interlayer in laminated glass. For example, Saad et al. (1995) investigated the behavior of PVB

following UV radiation and concluded that UV has a significant impact, showing that during UV irradiation of PVB, cross-linking predominates.

Andreozzi et al. (2015) investigated the effects of humidity, thermal cycles, and UV radiation on PVB, concluding that temperature had little to no impact, humidity impacted adhesion more than the bulk response, and UV had the most significant impact on the mechanical behavior. The UV caused a dramatic stiffening of the PVB. While stiffening might be considered beneficial in some cases, it can cause the PVB to exhibit brittle behavior, which is counter-productive for energy absorption. Stiffening also reduces adhesion, which is necessary for the interlayer to contain glass shards after the window break. In all three cases, following specimen conditioning, Andreozzi et al. (2015) measured rheological properties using an oscillatory test. Tensile tests, which are used in the study outlined in this paper, could produce new and possibly different conclusions than oscillatory tests.

Some authors studied the mechanisms of degradation of EVA and SG as well. Serafinavicius et al. (2014) subjected glass beams laminated with SG, PVB, EVA to a combination of humidity, high temperature, and UV radiation. All tests were carried out in a climatic chamber. The temperature levels + 200°C, + 300°C, + 400°C were controlled automatically at the set level for 24 hours for each temperature level, 72 hours in total loading time. Humidity inside the chamber was controlled at 50%. Long-term bending tests were carried out with the specimens supported at four-point bending. The results were compared in a load path diagram produced by creep four-point bending tests at various temperatures. It was found that temperature aging effects have the greatest impact on all

laminated glass specimens and the humidity aging effect has a minimal impact. The aging effect of UV radiation causes a slight hardening of the interlayer, and some deflection difference appears at a higher temperature +400°C. However, the combined effect of temperature, humidity, and UV has a similar impact as the UV radiation.

Delincé et al. (2007) investigated the effect of artificial weathering, particularly humidity and UV radiation, on shear-bond properties of PVB and SentryGlas® Plus (SGP) using different types of mechanical tests. These experiments aimed to compare local effects from shear tests to global effects from bending tests. Laminated glass plates measuring 300×300 mm were subjected to artificial weathering prior to drilling the cylindrical samples to be used in shear tests. Laminated glass plates of 1100×360 mm for bending tests were subjected to similar weathering exposures. For both types of artificial weathering, UV and humidity, evaluation of samples was made not less than 24 hours after the end of the weathering process, according to the ISO 12543-4. A visual evaluation of signs of delamination was done in all cases, and a measurement of the light transmittance before and after exposure to UV radiation was done only for 300×300 mm samples. No defect according to evaluation criteria of the standard was noticed for the tested samples. The main conclusion is that mechanical tests can be relevant to measure the effects of weathering on shear-bond properties, complementary to visual evaluation prescribed in standards, to calibrate design values on the basis of statistical analysis.

Butchart & Overend (2013) described the results of an experimental campaign of peeling tests. The peel tests were performed to investigate adhesion under different moisture levels. Peel tests were performed on specimens of PVB laminated between a layer of glass and a

layer of foil backing. The investigations show that in the presence of water, the adhesion between the glass and interlayer was less than half that observed in dry conditions.

Weller & Kothe (2011) carried out different aging scenarios on modified PVB, thermoplastic polyurethane (TPU), ionomer (SG), and EVA to assess the long-term stability, such as a temperature storage test, a climatic stress test, and a test under aggressive media and high irradiation. These ageing tests with small-scale test specimens affected both the appearance and the material properties. It was concluded that the best performance interlayer materials after the different aging tests are SG and a TPU. These materials are best suited for long-term use as a laminated glass interlayer for both indoor and outdoor applications.

Ensslen (2007) reported an extensive analysis of the behavior of laminated glass units subjected to weathering action: some specimens were subjected to UV radiation in a solarium, some underwent degradation cycles in temperature and humidity mixed conditions, some were simply exposed to the outdoor environmental weather for two years, in different climates. The comparison among the specimens artificially weathered and the ones exposed to the real weathering was made via monotonic shear tests. Experimental investigations showed that moisture penetration of the PVB interlayer on the glass edges has a negative impact on the durability of laminated glass. This results in an impairment of the shear stiffness as well as the bond strength. Aging of the interlayer due to UV radiation and high air temperatures, depending on its duration and intensity, leads to stiffening of the material properties, but not to impairment of the structural safety.

Antolinc et al. (2020) performed a three-point bending test on laminated glass at elevated temperature in an environmental chamber. The tested specimens were made of two fully tempered glass plates bonded with EVA and PVB interlayers. The tests were conducted at 23°C, 35°C, and 60°C after the specimens had reached the defined contact temperature. It was found that laminated glass with the EVA interlayer exhibits more favorable overall behavior at the elevated temperature in comparison to the specimen with the PVB interlayer. The only deficiency of the EVA interlayer is that it began to tear at the temperature of 60°C. Further research on the bending of laminated glass with smaller temperature steps is recommended, as well as at temperatures below room and sub-zero temperatures.

Martín et al. (2020) conducted high strain rate tests on seven different polymer interlayers, including three different PVB products, one SG product, two EVA products, and a TPU product at three different strain rates. The mechanical and optical properties of unaged specimens are compared with specimens exposed to thermal cycles, high temperatures, and moisture. The unaged specimens of PVB and SG had the highest stiffness, EVA had the highest ductility, and PVB and SG had the highest tensile strength. In addition, EVA and TPU were less affected by aging factors and strain rate.

3 STRAIN RATE EFFECTS ON MECHANICAL RESPONSE OF POLYMER INTERLAYERS

3.1 INTRODUCTION

The material behavior of polymer interlayers is highly strain-rate dependent. Throughout this study, results will be categorized by "static" or "dynamic". Static tests were performed using a servo-hydraulic machine and have strain rates less than 1 s^{-1}. Dynamic tests were performed using a drop-weight machine and have a strain rate between 30 and 100 s^{-1}. The static and dynamic test procedures are outlined in the following section. This chapter will also describe the data analysis procedures and provide a brief study of the behavior of polymer interlayers at various quasi-static strain rates. This strain rate study serves to better characterize the effects of strain rate on the material behavior.

3.2 TEST PROCEDURES

3.2.1 Quasi-Static Tensile Test

This section describes the quasi-static tensile test specimen preparation, test setup, and test procedure. The static specimen dimensions were chosen following ASTM D638-14, 2014 Type IV (Figure 3). Specimens were cut using steel dies and a hydraulic press (Figure 4). The test was performed using a servo-hydraulic quasi-static tensile test machine (Figure 6). The specimen is labeled with two dots spaced 1-inch apart along the gage-length. For EVA specimens, a dot is drawn on a small strip of paper and attached to the sample using

paper clips (Figure 5). This method was adopted because the dots drawn on the EVA sample would disappear as the sample reached large deformations. The specimen is secured in the machine with two metal grips (Figure 7). The test is run at various strain rates to determine the slow strain rate effect. The computer records load data from a 2-kip load cell at an interval of 0.01 seconds while a camera captures the entire event. This camera footage is later converted to pictures, and the software PhotoTrack (Appendix) is used to determine the relative displacement between the two dots (Figure 8). The load-displacement data can then be used to develop a stress-strain diagram, which will be helpful for material behavior comparison throughout this thesis.

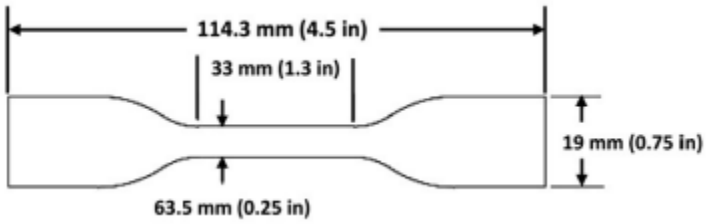

Figure 3: ASTM D638-14 Type IV Specimen Dimensions

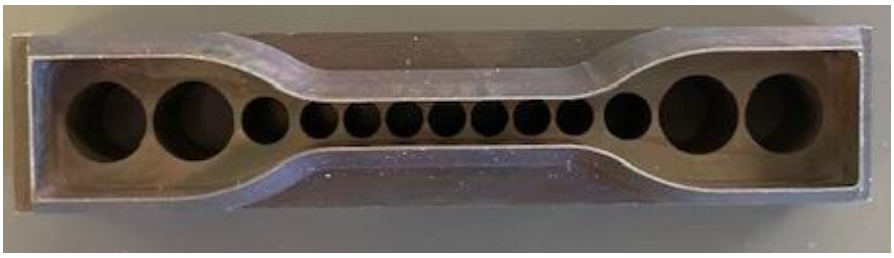

Figure 4: Steel Die for Static Test Specimens

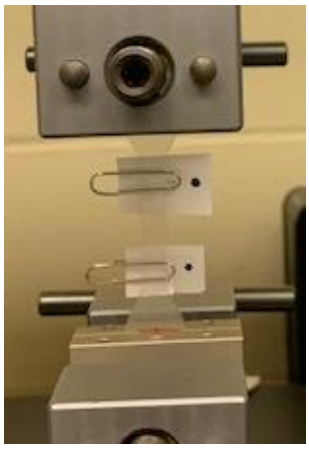

Figure 5: Paper Clip Method for EVA Specimens

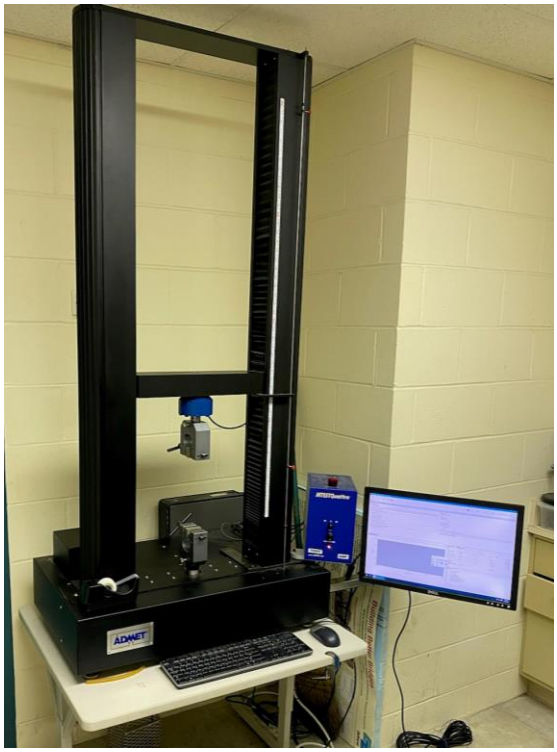

Figure 6: Servo-Hydraulic Quasi-Static Tensile Test Machine

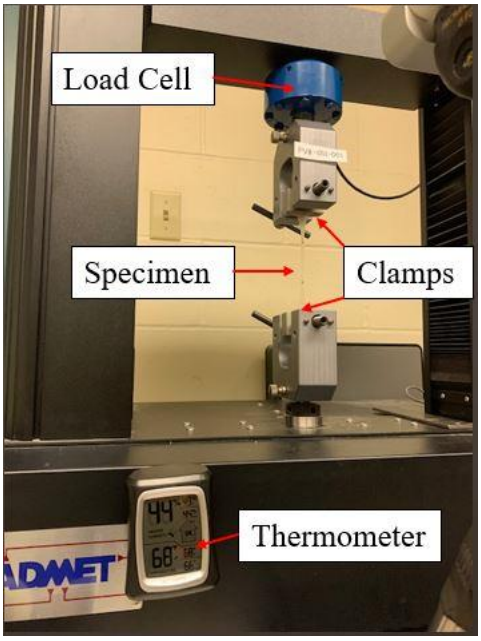

Figure 7: Annotation of Quasi-Static Tensile Test Machine Parts

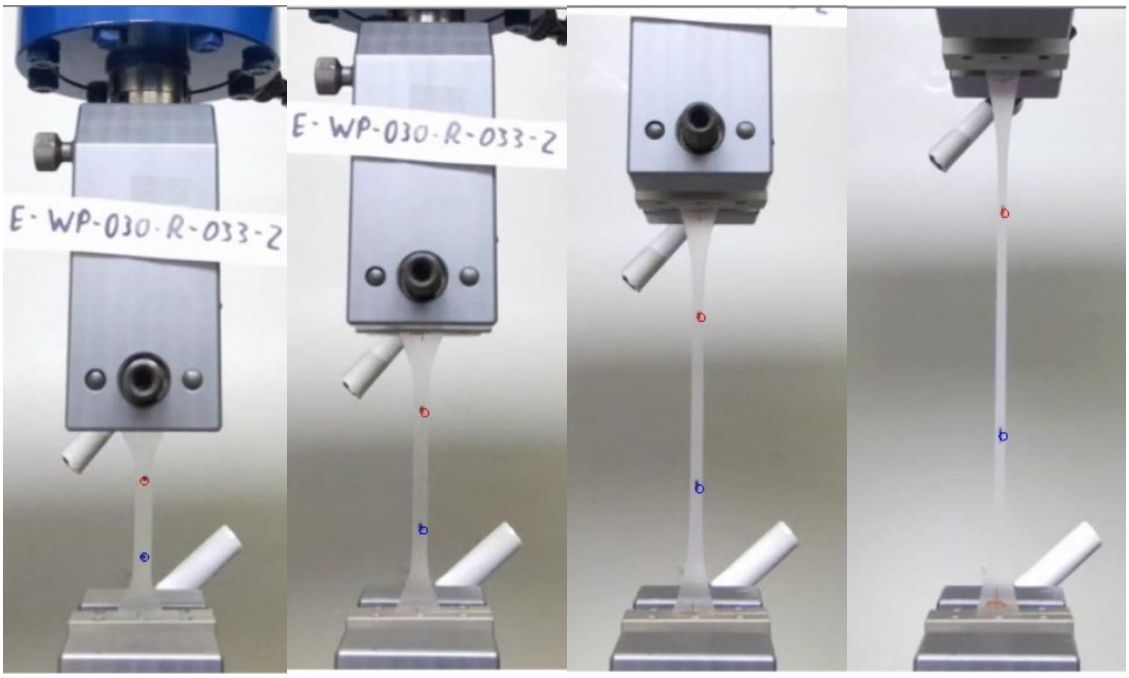

Figure 8: PhotoTrack Dot-Tracking to Determine Strain

3.2.2 Dynamic Drop-Weight Test

This section describes the dynamic drop-weight test specimen preparation, test setup, and test procedure. The dynamic specimen dimensions were chosen following ASTM D638-14 (2014) Type 1 with some modifications to increase the area of the end tabs to mitigate tear-out failures (Figure 9). Specimens were cut using steel dies and a hydraulic press (Figure 10). The specimens were labeled with two dots spaced one inch apart along the gage length. The end tabs were strengthened by super-gluing aluminum tabs to either side (Figure 11). A drop-weight machine was used to achieve the high strain rates required in dynamic testing (Figure 12). The drop-weight machine works by releasing a weight from a height specified by the user. As the weight falls, two striker rods hit an anvil that is attached to the specimen. The anvil accelerates downward with the weight, pulling the specimen in tension. Load and time data is recorded from a 500-pound load cell, and a high-speed camera captures the entire event (Figure 13). This camera footage is later converted to pictures, and the software PhotoTrack is used to determine the relative displacement between the two dots. The load-displacement data can then be used to develop a stress-strain diagram. For a more detailed description of these test procedures, please refer to the papers of Jonathan Knight and Mahmoud Nawar (Nawar, 2016; Knight, 2020).

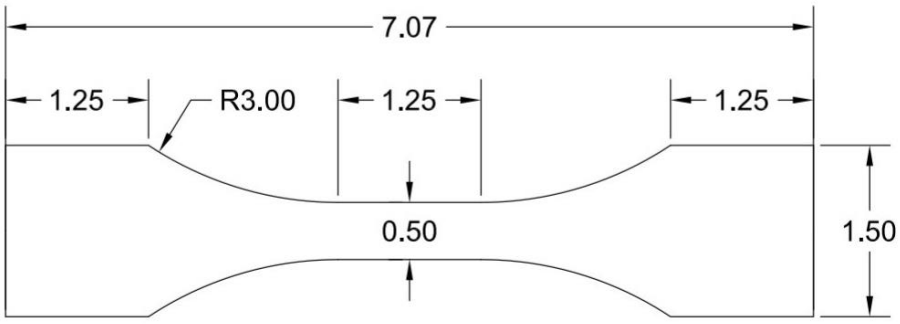

Figure 9: ASTM D638-14 Type 1 Specimen with End Tab Modifications

Figure 10: Steel Die for Dynamic Test Specimens

Figure 11: Dynamic Test Specimen Preparation

Figure 12: Dynamic Drop-Weight Machine

Figure 13: High Speed Camera

3.3 STRAIN RATE EFFECT

3.3.1 Data Analysis Procedures

The data collected for quasi-static and dynamic tests included load and displacement. The displacement was measured using PhotoTrack and converted to strain using Equation 1, where L is the initial length in pixels.

Equation 1: Strain Calculation

$$\dot{\varepsilon} = \frac{y}{L} - 1$$

The load-time data was recorded by the load cell and converted to stress using Equation 2, where P is the load and A is the cross-sectional area of the specimen.

Equation 2: Stress Calculation

$$\sigma = \frac{P}{A}$$

Stress-strain curves were graphed using the software DPlot. Important properties are presented in tables throughout the results. These important points include experimental strain rate, pseudo-yield, failure, initial and secondary moduli, and strain energy. The experimental strain rate for quasi-static tests was found as the grip displacement rate (in/min) divided by 60 (sec/min). The experimental strain rate for dynamic tests was taken as the slope of a linear regression of the strain-time curve; for example, in Figure 14 the experimental strain rate is 27.9 s^{-1}. The pseudo-yield refers to the point of abrupt change in the modulus. The initial modulus is taken as the average slope of the curve up to and including the pseudo-yield. The secondary modulus is the average slope of the curve after the pseudo-yield. These three properties are demonstrated in Figure 15. The initial modulus for static testing of EVA, however, is taken as the average slope of the curve up to a strain of 0.15 in/in. This was determined as the most linear portion of the curve prior to the pseudo-yield. Strain energy represents the total energy that could be absorbed by the material and is calculated as the total area under the stress-strain curve.

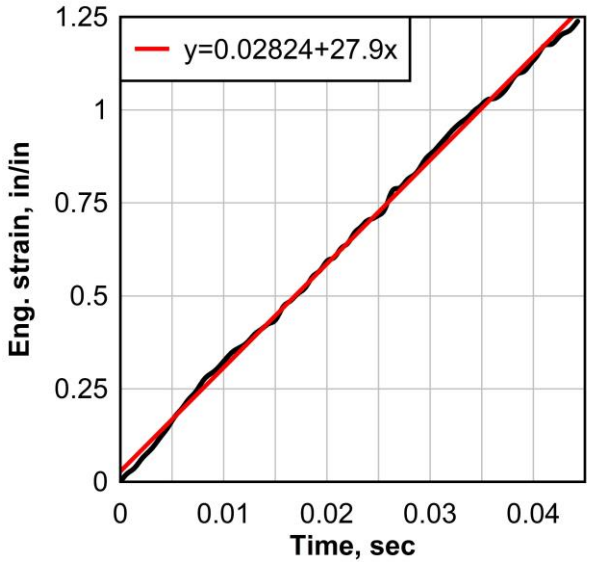

Figure 14: Dynamic Strain Rate Determination

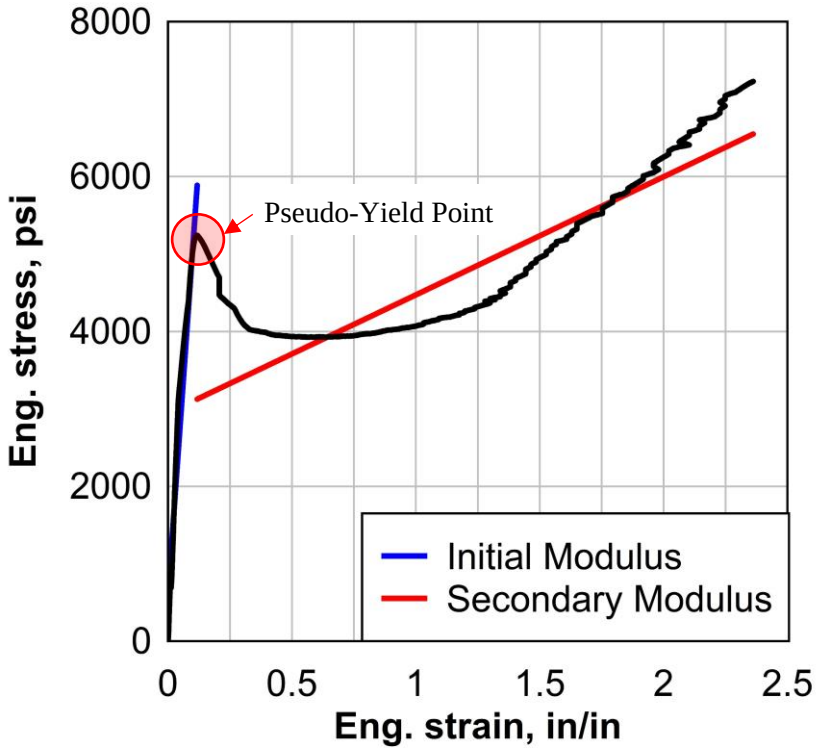

Figure 15: Demonstration of Moduli and Pseudo-Yield

3.3.2 Low Strain-Rate

Polymers are viscoelastic materials, which means the mechanical behavior will be strain rate dependent. This study was done to determine the effect strain rate within the quasi-static range and compare to the effect of strain rate within the intermediate range. The low strain-rate tests were performed using the quasi-static tensile test machine. Tests were performed on Saflex Standard Clear PVB, EVGuard EVA, SG5000, and SG6000. Three strain rates, 0.033 s^{-1}, 0.083 s^{-1}, and 0.167 s^{-1}, were chosen. The test machine grip displacement was set to 2 in/min, 5 in/min, or 10 in/min to achieve the corresponding strain rate. Results are shown as stress-strain curves. Each curve is the average of five individual tests. The tables below each figure give the important properties for each of the five tests as well as an average of these values.

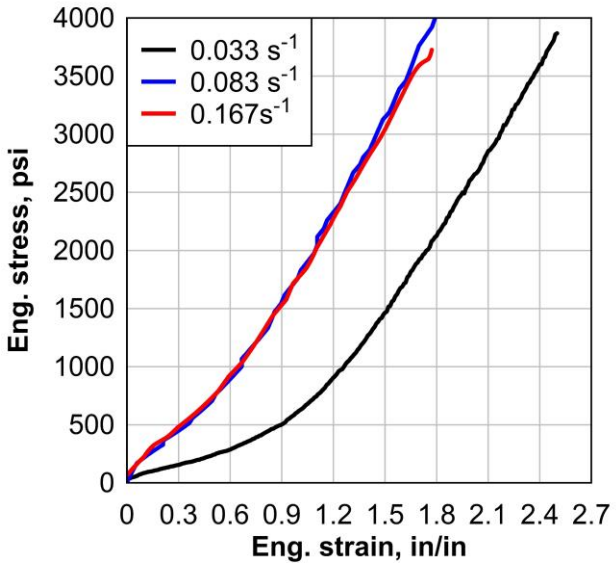

Figure 16: PVB Strain Rate Comparison

Table 1: PVB 0.033 s^{-1} Strain Rate Test Results

PVB 2 in/min							
No.	Specimen	Temperature, °F	Experimental Strain Rate, $\dot{\varepsilon}_E$ (s^{-1})	Failure Stress, σ_f (psi)	Failure Strain, ε_f (in/in)	Avg. Modulus, E_{avg} (psi)	Strain Energy, U (psi·in/in)
1	E-P-030-R-033-1	69	0.033	3741	2.626	1493	3511
2	E-P-030-R-033-2	69	0.033	3736	2.665	1481	3502
3	E-P-030-R-033-3	69	0.033	3821	2.782	1450	3598
4	E-P-030-R-033-4	69	0.033	3890	2.831	1407	3596
5	E-P-030-R-033-5	69	0.033	3255	2.550	1277	2730
Avg.		**69**	**0.033**	**3689**	**2.691**	**1422**	**3387**

Table 2: PVB 0.083 s^{-1} Strain Rate Test Results

PVB 5 in/min							
No.	Specimen	Temperature, °F	Experimental Strain Rate, $\dot{\varepsilon}_E$ (s^{-1})	Failure Stress, σ_f (psi)	Failure Strain, ε_f (in/in)	Avg. Modulus, E_{avg} (psi)	Strain Energy, U (psi·in/in)
1	E-P-030-R-083-1	66	0.083	3839	1.772	2156	3019
2	E-P-030-R-083-2	66	0.083	4154	1.930	2161	3609
3	E-P-030-R-083-3	66	0.083	3619	1.740	2135	2678
4	E-P-030-R-083-4	66	0.083	3564	1.559	2208	2544
5	E-P-030-R-083-5	66	0.083	4120	1.959	2128	3402
Avg.		**66**	**0.083**	**3859**	**1.792**	**2158**	**3050**

Table 3: PVB 0.167 s^{-1} Strain Rate Test Results

PVB 10 in/min							
No.	Specimen	Temperature, °F	Experimental Strain Rate, $\dot{\varepsilon}_E$ (s^{-1})	Failure Stress, σ_f (psi)	Failure Strain, ε_f (in/in)	Avg. Modulus, E_{avg} (psi)	Strain Energy, U (psi·in/in)
1	E-P-030-R-167-1	66	0.167	4185	1.79	2325	3318
2	E-P-030-R-167-2	66	0.167	4211	1.846	2333	3362
3	E-P-030-R-167-3	66	0.167	4088	1.806	2276	3099
4	E-P-030-R-167-4	66	0.167	4101	1.844	2258	3345
5	E-P-030-R-167-5	66	0.167	4326	1.956	2248	3463
Avg.		**66**	**0.167**	**4182**	**1.848**	**2288**	**3317**

Table 4: PVB 45 s^{-1} Strain Rate Test Results

PVB Dynamic										
No.	Specimen	Temperature, °F	Experimental Strain Rate, $\dot{\varepsilon}_E$ (s^{-1})	Pseudo-yield Stress, $\sigma_{ps,y}$ (psi)	Pseudo-yield Strain, $\varepsilon_{ps,y}$ (in/in)	Failure Stress, σ_f (psi)	Failure Strain, ε_f (in/in)	Initial Modulus, E_{ini} (psi)	Secondary Modulus, E_{sec} (psi)	Strain Energy, U (psi·in/in)
1	E-P-030-R68-045-1	68	43.38	2585	0.124	4799	1.746	24,440	1592	5380
2	E-P-030-R68-045-2	68	42.36	2274	0.114	4340	1.651	24,007	1690	4665
3	E-P-030-R68-045-3	68	41.18	2163	0.085	4599	1.622	30,626	1607	4843
4	E-P-030-R68-045-4	68	41.54	2607	0.137	4729	1.650	20,041	1659	5069
5	E-P-030-R68-045-5	68	42.15	2036	0.070	4562	1.800	36,939	1687	5601
Avg.		**68**	**42.12**	**2333**	**0.106**	**4606**	**1.694**	**27,211**	**1647**	**5112**

The average curves for each quasi-static strain rate, displayed in Figure 16, show that the material stiffened with higher strain rate. This affect is typical for PVB and has been shown in previous works, including the study done by (Zhang et al., 2015). It is interesting that

the average modulus, which is representative of stiffness, increased by 52% from 0.033 s^{-1} to 0.083 s^{-1}, but only increased by 6% from 0.083 s^{-1} to 0.167 s^{-1}(Table 1, Table 2, Table 3). The strain energy is comparable for the three quasi-static tests, but the dynamic test strain energy increases by a minimum of 50% (Table 4). An increase in strain energy at high strain rates is a desirable quality for blast scenarios because energy absorption is the most important characteristic.

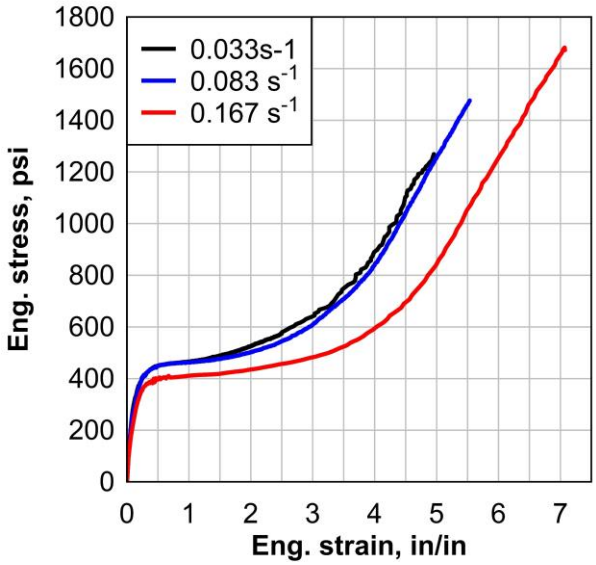

Figure 17: EVA (EVGuard) Strain Rate Comparison

Table 5: EVA 0.033 s^{-1} Strain Rate Results

EVA 2 in/min									
No.	Specimen	Temperature, °F	Experimental Strain Rate, $\dot{\varepsilon}_E$ (s^{-1})	Pseudo-yield Stress, $\sigma_{ps,y}$ (psi)	Pseudo-yield Strain, $\varepsilon_{ps,y}$ (in/in)	Failure Stress, σ_f (psi)	Failure Strain, ε_f (in/in)	Initial Modulus, E_{ini} (psi)	Strain Energy, U (psi·in/in)
1	S-E-030-R-033-1	66	0.033	449.6	0.454	1642	4.955	2245	3682
2	S-E-030-R-033-2	66	0.033	446.4	0.489	1770	6.426	2182	5149
3	S-E-030-R-033-3	66	0.033	452.8	0.452	1670	6.197	2018	4777
4	S-E-030-R-033-4	66	0.033	449.6	0.453	1868	6.149	2293	4982
5	S-E-030-R-033-5	66	0.033	440.0	0.485	2063	7.135	2552	6077
Avg.		**66**	**0.033**	**447.7**	**0.467**	**1803**	**6.172**	**2258**	**4933**

Table 6: EVA 0.083 s^{-1} Strain Rate Results

EVA 5 in/min									
No.	Specimen	Temperature, °F	Experimental Strain Rate, $\dot{\varepsilon}_E$ (s^{-1})	Pseudo-yield Stress, $\sigma_{ps,y}$ (psi)	Pseudo-yield Strain, $\varepsilon_{ps,y}$ (in/in)	Failure Stress, σ_f (psi)	Failure Strain, ε_f (in/in)	Initial Modulus, E_{ini} (psi)	Strain Energy, U (psi·in/in)
1	S-E-030-R-083-1	66	0.083	433.0	0.494	1823	5.535	2467	4426
2	S-E-030-R-083-2	66	0.083	427.6	0.496	1827	9.603	1789	7767
3	S-E-030-R-083-3	66	0.083	452.8	0.487	1910	6.836	2389	5732
4	S-E-030-R-083-4	66	0.083	468.1	0.438	1909	5.979	2562	5059
5	S-E-030-R-083-5	66	0.083	465.2	0.493	1887	5.733	2230	4848
Avg.		**66**	**0.083**	**449.3**	**0.482**	**1871**	**6.737**	**2287**	**5566**

Table 7: EVA 0.167 s^{-1} Strain Rate Results

EVA 10 in/min									
No.	Specimen	Temperature, °F	Experimental Strain Rate, $\dot{\varepsilon}_E$ (s^{-1})	Pseudo-yield Stress, $\sigma_{ps,y}$ (psi)	Pseudo-yield Strain, $\varepsilon_{ps,y}$ (in/in)	Failure Stress, σ_f (psi)	Failure Strain, ε_f (in/in)	Initial Modulus, E_{ini} (psi)	Strain Energy, U (psi·in/in)
1	S-E-030-R-167-1	66	0.167	395.4	0.479	1797	8.166	1650	6146
2	S-E-030-R-167-2	66	0.167	402.7	0.460	1751	7.075	1808	5118
3	S-E-030-R-167-3	66	0.167	405.2	0.486	1839	7.169	2180	5612
4	S-E-030-R-167-4	66	0.167	414.2	0.483	1766	7.331	1956	5769
5	S-E-030-R-167-5	66	0.167	381.3	0.493	1801	6.942	1800	5109
Avg.		**66**	**0.167**	**400**	**0.480**	**1791**	**7.337**	**1879**	**5551**

The property that changes consistently with the increase in strain rate is the failure strain. The failure strain increased proportional to the strain rate. The pseudo-yield and initial modulus are nearly identical between the 0.033 s^{-1} and 0.83 s^{-1} strain rates (Table 5, Table 6). The faster strain rate of 0.167 s^{-1}, however, has a lower pseudo-yield and a lower initial modulus, demonstrating that the material shows less stiffness with an increased strain rate (Table 7). The strain energy is higher than that of PVB because the EVA achieves such extreme values of failure strain; 2 to 6 times that of PVB. These high strains are not serviceable because the glass shards would cut through the polymer interlayer before achieving the maximum strain. Because of this, the large strain energy of EVA is not all useful. The maximum strain experienced by an LG window before the glass shards break through the polymer interlayer is likely somewhere around 2 in/in. This number, however, is not verified. As a demonstration, the strain energy up to a strain of 2 in/in for EVA at a strain rate of 0.033 s^{-1} is 898 psi·in/in, which is only 18% of the total strain energy (Table 5). In conclusion, though EVA appears to have many advantageous properties for

laminated glass, the useable portion of the stress-strain behavior does not make EVA as desirable.

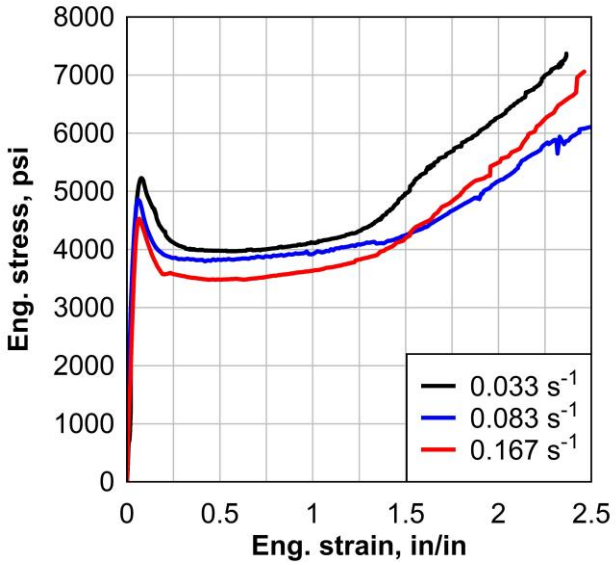

Figure 18: SG5000 Strain Rate Comparison

Table 8: SG5000 0.033 s^{-1} Strain Rate Results

SG5000 2 in/min										
No.	Specimen	Temperature, °F	Experimental Strain Rate, $\dot{\varepsilon}_E$ (s^{-1})	Pseudo-yield Stress, $\sigma_{ps,y}$ (psi)	Pseudo-yield Strain, $\varepsilon_{ps,y}$ (in/in)	Failure Stress, σ_f (psi)	Failure Strain, ε_f (in/in)	Initial Modulus, E_{ini} (psi)	Secondary Modulus, E_{sec} (psi)	Strain Energy, U (psi·in/in)
1	K-S5-035-R-033-1	66	0.033	5231	0.075	7384	2.365	77150	1549	11530
2	K-S5-035-R-033-2	66	0.033	5302	0.077	7286	2.318	75500	1465	11340
3	K-S5-035-R-033-3	66	0.033	5242	0.118	7229	2.362	44970	1525	11448
4	K-S5-035-R-033-4	66	0.033	5239	0.078	7603	2.419	76890	1618	11880
5	K-S5-035-R-033-5	66	0.033	5146	0.076	7106	2.385	74070	1388	11433
Avg.		**66**	**0.033**	**5232**	**0.085**	**7322**	**2.370**	**69716**	**1509**	**11526**

Table 9: SG5000 0.083 s^{-1} Strain Rate Results

SG5000 5 in/min										
No.	Specimen	Temperature, °F	Experimental Strain Rate, $\dot{\varepsilon}_E$ (s^{-1})	Pseudo-yield Stress, $\sigma_{ps,y}$ (psi)	Pseudo-yield Strain, $\varepsilon_{ps,y}$ (in/in)	Failure Stress, σ_f (psi)	Failure Strain, ε_f (in/in)	Initial Modulus, E_{ini} (psi)	Secondary Modulus, E_{sec} (psi)	Strain Energy, U (psi·in/in)
1	K-S5-035-R-083-1	66	0.083	4528	0.066	6771	2.543	73890	1432	11254
2	K-S5-035-R-083-2	66	0.083	5187	0.066	7067	2.464	76540	1267.0	11704
3	K-S5-035-R-083-3	66	0.083	4534	0.047	6604	2.489	102600	1228	10805
4	K-S5-035-R-083-4	66	0.083	1814	0.035	4450	2.204	51810	1336	5267
5	K-S5-035-R-083-5	66	0.083	4679	0.073	6702	2.420	69050	1329	10547
Avg.		**66**	**0.083**	**4732**	**0.063**	**6786**	**2.479**	**80520**	**1314**	**11078**

Table 10: SG5000 0.167 s^{-1} Strain Rate Results

SG5000 10 in/min										
No.	Specimen	Temperature, °F	Experimental Strain Rate, $\dot{\varepsilon}_E$ (s^{-1})	Pseudo-yield Stress, $\sigma_{ps,y}$ (psi)	Pseudo-yield Strain, $\varepsilon_{ps,y}$ (in/in)	Failure Stress, σ_f (psi)	Failure Strain, ε_f (in/in)	Initial Modulus, E_{ini} (psi)	Secondary Modulus, E_{sec} (psi)	Strain Energy, U (psi·in/in)
1	K-S5-035-R-167-1	66	0.167	5056	0.018	6605	2.617	297500	1049	12002
2	K-S5-035-R-167-2	66	0.167	4637	0.072	6078	2.543	71410	1032.0	10475
3	K-S5-035-R-167-3	66	0.167	5125	0.062	6286	2.325	93430	815.2	10427
4	K-S5-035-R-167-4	66	0.167	4865	0.054	6057	2.492	93420	1028	10772
5	K-S5-035-R-167-5	66	0.167	5444	0.054	6278	2.324	105900	824.8	10832
Avg.		**66**	**0.167**	**5025**	**0.052**	**6261**	**2.460**	**132332**	**949.8**	**10902**

Table 11: SG5000 45 s^{-1} Strain Rate Results

SG5000 Dynamic										
No.	Specimen	Temperature, °F	Experimental Strain Rate, $\dot{\varepsilon}_E$ (s^{-1})	Pseudo-yield Stress, $\sigma_{ps,y}$ (psi)	Pseudo-yield Strain, $\varepsilon_{ps,y}$ (in/in)	Failure Stress, σ_f (psi)	Failure Strain, ε_f (in/in)	Initial Modulus, E_{ini} (psi)	Secondary Modulus, E_{sec} (psi)	Strain Energy, U (psi·in/in)
1	K-S5-035-R-045-1	68	38.96	6777	0.149	5757	1.544	75,761	-202	8885
2	K-S5-035-R-045-2	68	44.94	6918	0.172	5850	1.187	63,167	-573	6832
3	K-S5-035-R-045-3	68	50.21	6551	0.145	5030	1.153	56,275	-1177	5984
4	K-S5-035-R-045-4	68	40.13	6383	0.187	5687	1.437	46,349	-411	7826
5	K-S5-035-R-045-5	68	41.48	6642	0.134	5701	1.436	69,830	-421	8093
Avg.		**68**	**43.14**	**6654**	**0.157**	**5605**	**1.351**	**62,276**	**-557**	**7524**

Table 8 show the important properties of SG5000 for three quasi-static strain rates. Table 11 shows dynamic results of the same material for comparison. The steady increase in initial modulus for the quasi-static strain rates shows that SG stiffens with increased strain rate (Table 8, Table 9, Table 10). This is consistent with viscoelastic material behavior. The failure stress and strain energy both decrease with increasing strain rate. This behavior is very apparent when comparing the quasi-static tests to the 45 s^{-1} strain rate, which has a significant reduction in failure stress, failure strain, and strain energy (Table 11). The dynamic behavior of the material is more brittle while the static behavior is more ductile. In comparison to both PVB and EVA, the SG achieves significantly higher strength and energy absorption. The SG also has a higher stiffness as represented by the initial modulus which is one to two orders of magnitude larger than that of PVB and EVA.

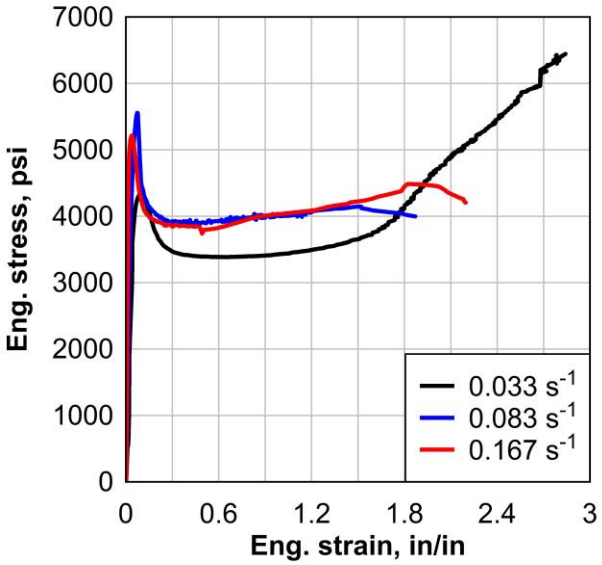

Figure 19: SG6000 Strain Rate Comparison

Table 12: SG6000 0.033 s^{-1} Strain Rate Results

SG6000 2 in/min										
No.	Specimen	Temperature, °F	Experimental Strain Rate, $\dot{\varepsilon}_E$ (s^{-1})	Pseudo-yield Stress, $\sigma_{ps,y}$ (psi)	Pseudo-yield Strain, $\varepsilon_{ps,y}$ (in/in)	Failure Stress, σ_f (psi)	Failure Strain, ε_f (in/in)	Initial Modulus, E_{ini} (psi)	Secondary Modulus, E_{sec} (psi)	Strain Energy, U (psi·in/in)
1	K-S6-035-R-033-1	66	0.033	4389	0.100	6516	2.801	47990	1160	11676
2	K-S6-035-R-033-2	66	0.033	4296	0.096	6520	2.726	49680	1170	11126
3	K-S6-035-R-033-3	66	0.033	4453	0.123	6726	2.946	47950	1187	12294
4	K-S6-035-R-033-4	66	0.033	4403	0.100	6669	2.980	54010	1143	12674
5	K-S6-035-R-033-5	66	0.033	4400	0.082	6300	2.813	66410	1094	11565
Avg.		**66**	**0.033**	**4388.2**	**0.100**	**6546**	**2.853**	**53208**	**1151**	**11867**

Table 13: SG6000 0.083 s^{-1}Strain Rate Results

SG6000 5 in/min										
No.	Specimen	Temperature, °F	Experimental Strain Rate, $\dot{\varepsilon}_E$ (s^{-1})	Pseudo-yield Stress, $\sigma_{ps,y}$ (psi)	Pseudo-yield Strain, $\varepsilon_{ps,y}$ (in/in)	Failure Stress, σ_f (psi)	Failure Strain, ε_f (in/in)	Initial Modulus, E_{ini} (psi)	Secondary Modulus, E_{sec} (psi)	Strain Energy, U (psi·in/in)
1	K-S6-035-R-083-1	66	0.083	5283	0.072	5690	2.957	77310	319.4	11801
2	K-S6-035-R-083-2	66	0.083	5384	0.051	5992	1.888	108000	674.2	8802
3	K-S6-035-R-083-3	66	0.083	5272	0.105	5165	2.554	53330	255.8	9637
4	K-S6-035-R-083-4	66	0.083	5255	0.091	5548	2.635	60090	307.5	10027
5	K-S6-035-R-083-5	66	0.083	5222	0.079	4215	2.138	63820	244.7	8635
Avg.		**66**	**0.083**	**5283**	**0.080**	**5322**	**2.434**	**72510**	**360.3**	**9780**

Table 14: SG6000 0.167 s^{-1} Strain Rate Results

SG6000 10 in/min										
No.	Specimen	Temperature, °F	Experimental Strain Rate, $\dot{\varepsilon}_E$ (s^{-1})	Pseudo-yield Stress, $\sigma_{ps,y}$ (psi)	Pseudo-yield Strain, $\varepsilon_{ps,y}$ (in/in)	Failure Stress, σ_f (psi)	Failure Strain, ε_f (in/in)	Initial Modulus, E_{ini} (psi)	Secondary Modulus, E_{sec} (psi)	Strain Energy, U (psi·in/in)
1	K-S6-035-R-167-1	66	0.167	5288	0.020	5929	2.197	295100	650.5	10221
2	K-S6-035-R-167-2	66	0.167	5386	0.040	6169	2.240	149300	761.2	10718
3	K-S6-035-R-167-3	66	0.167	5419	0.019	5529	3.000	308200	333.5	11911
4	K-S6-035-R-167-4	66	0.167	5169	0.041	4610	3.250	143000	74.9	12523
5	K-S6-035-R-167-5	66	0.167	5094	0.035	4043	3.067	161700	52.6	11217
Avg.		**66**	**0.167**	**5271**	**0.031**	**5256**	**2.751**	**211460**	**374.5**	**11318**

Table 15: SG6000 45 s^{-1} Strain Rate Results

SG6000 Dynamic										
No.	Specimen	Temperature, °F	Experimental Strain Rate, $\dot{\varepsilon}_E$ (s^{-1})	Pseudo-yield Stress, $\sigma_{ps,y}$ (psi)	Pseudo-yield Strain, $\varepsilon_{ps,y}$ (in/in)	Failure Stress, σ_f (psi)	Failure Strain, ε_f (in/in)	Initial Modulus, E_{ini} (psi)	Secondary Modulus, E_{sec} (psi)	Strain Energy, U (psi·in/in)
1	K-S6-035-R-045-1	68	45.78	7424	0.187	6474	1.555	48,382	-289	9740
2	K-S6-035-R-045-2	68	47.84	7357	0.148	6580	1.742	58,624	-267	10,964
3	K-S6-035-R-045-3	69	46.66	7173	0.105	5457	2.003	96,322	-461	11,392
4	K-S6-035-R-045-4	69	49.18	7140	0.117	6190	1.793	66,704	-273	10,973
5	K-S6-035-R-045-5	69	50.17	7248	0.208	6394	1.559	42,946	-314	9762
Avg.		**68.6**	**47.93**	**7268**	**0.153**	**6219**	**1.730**	**62,596**	**-321**	**10,566**

The stiffening behavior of polymer materials with increasing strain rate is very apparent in the SG6000 tests, with an initial modulus at a strain rate of 0.167 s^{-1} that is nearly four times that at a rate of 0.033 s^{-1} (Table 8, Table 10). One interesting visual observation from these tests was that SG6000 frequently had a very obvious necking throughout part of the gage length (Figure 20). In general, the SG6000 and SG5000 exhibit similar behavior with high strength, high strain energy, and a high initial modulus to a very distinct pseudo-yield point.

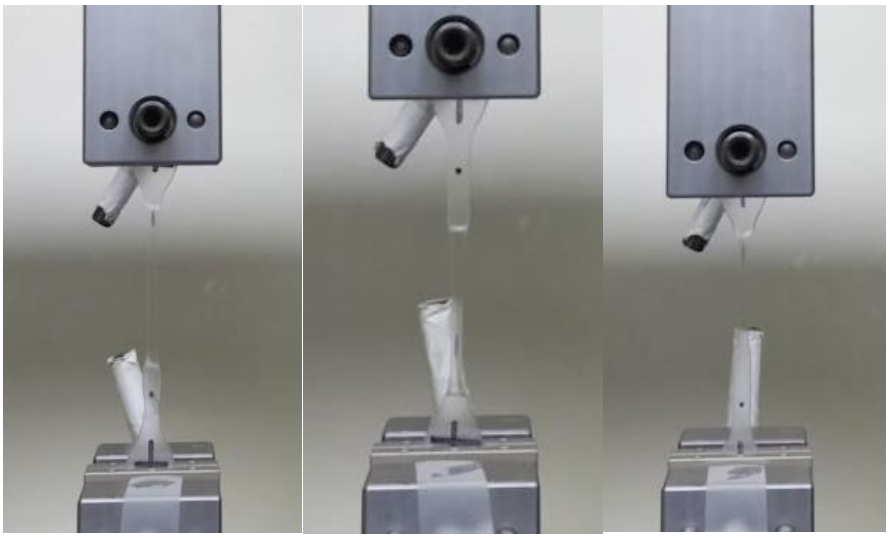

Figure 20: SG6000 Necking

4 EXPERIMENTAL EVALUATION OF ENVIRONMENTAL EFFECTS

4.1 INTRODUCTION

Weathering has a significant impact on the mechanical behavior of PVB, SG, and EVA. The following section will describe the test procedures for outdoor weathering and water immersion, the scope of testing performed for this thesis, the results of that testing, and a discussion of the conclusions that can be drawn.

4.2 TEST PROCEDURES

4.2.1 Outdoor Weathering Test

The following procedure and test plan is used for outdoor weathering of polymers. The procedure was developed following ASTM D1435 (2013) and ASTM G7 (2013). The test rack is oriented vertically, 90 degrees from the ground surface (Figure 21). Sheets of EVA, PVB, and SG measuring 12X12 inch are attached to the test rack with adhesive. Half the sheets are placed between two 1/4-inch-thick panes of glass and half are attached without glass. This will help characterize the effects of glass on the aging of polymer interlayer materials. Instruments collect climatological data including ambient temperature, relative humidity, and total solar radiation (Figure 22). These instruments are set up less than 100 yards from the rack and at the same orientation as the sample sheets. Samples are being tested after exposure periods of 1, 3, 6, 9, and 12 months. 5 samples each shall be tested

statically and dynamically (strain rate 45 s^{-1}). Table 16 outlines the tests to be performed and highlights the results that will be presented in this paper.

Figure 21: Outdoor Weathering Rack

Figure 22: Outdoor Weathering Instruments

Table 16: Outdoor Weathering Test Matrix

Time (months)	Date	Polymer	Thickness (in)	Strain Rate			
				Static		Dynamic	
				In-Glass	Out-of-Glass	In-Glass	Out-of-Glass
1	2/8/2021	Saflex Standard Clear	0.03	5	5	5	5
		Evguard EVA	0.03	5	5	5	5
		SG6000	0.035	5	5	5	5
3	4/8/2021	Saflex Standard Clear	0.03	5	5	5	5
		Evguard EVA	0.03	5	5	5	5
		SG6000	0.035	5	5	5	5
6	7/8/2021	Saflex Standard Clear	0.03	5	5	5	5
		Evguard EVA	0.03	5	5	5	5
		SG6000	0.035	5	5	5	5
9	10/8/2021	Saflex Standard Clear	0.03	5	5	5	5
		Evguard EVA	0.03	5	5	5	5
		SG6000	0.035	5	5	5	5
12	1/8/2022	Saflex Standard Clear	0.03	5	5	5	5
		Evguard EVA	0.03	5	5	5	5
		SG6000	0.035	5	5	5	5

4.2.2 Water Immersion Test

This section will describe the water immersion test specimen preparation, test setup, and test procedure. The water absorption for each material can be determined following the standards ASTM D570-98 and ISO 62. In order to perform quasi-static and dynamic tests on the material after immersion, the 60X60 mm test specimen specified in the standards is not acceptable. Therefore, 5×1.5 inch and 9×2 inch rectangular specimens are used for quasi-static and dynamic testing respectively. The specimens are weighed on a scale to the nearest 0.1mg (Figure 23), then placed in a thermostatic water bath (Figure 24). The water bath is filled with distilled water at a temperature of 73.4$\pm$1.8°F until the water level is approximately one inch above the specimens (Figure 25). The specimens are removed and weighed to the nearest 0.1mg at intervals of 1, 2, 4, 8, 16, 24, 48, 96, and 168 hours following the procedure used by (Centelles et al., 2020). After 168 hours, the specimens are dried in an oven at 40°C for 24 hours then re-weighed to verify total moisture content

(Figure 26, Figure 27). The specimens are kept in a desiccator while awaiting testing to keep out moisture (Figure 28).

Following the water immersion procedure, the standard testing coupons described in Sections 3.2.1. and 3.2.2. are cut from the rectangular specimens and tested following the standard procedures outlined therein.

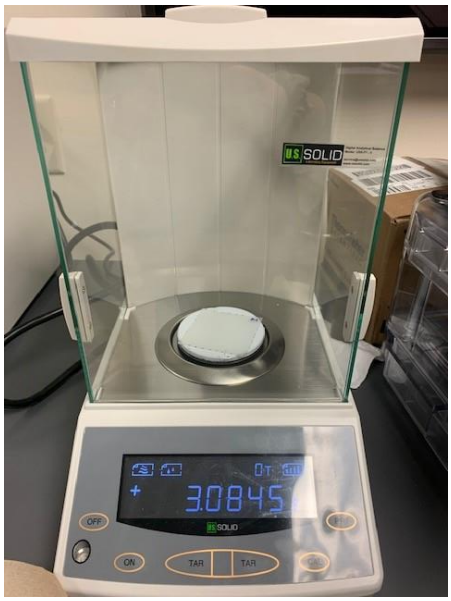

Figure 23: Scale Capable of Weighing to the Nearest 0.1mg

Figure 24: Thermostatic Water Bath

Figure 25: Water Bath from Above with Static Specimens

Figure 26: Drying Oven

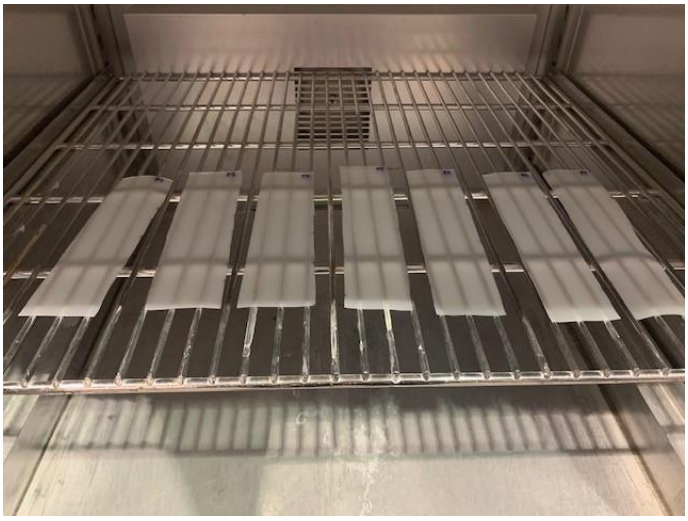

Figure 27: Oven with Dynamic PVB Specimens

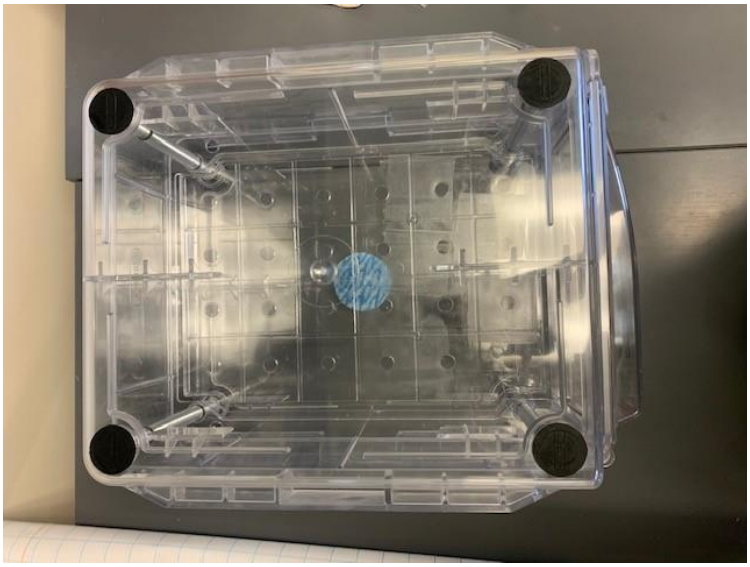

Figure 28: Desiccator from Above with Desiccant Packet

4.3 OUTDOOR WEATHERING RESULTS AND DISCUSSION

The results of the first month of outdoor weathering are presented in this section. A summary of these results with qualitative comparison is shown in Table 39. Materials tested include Saflex Standard Clear RA41 PVB, Evguard EVA, and Kuraray SG6000.

Static **Dynamic**

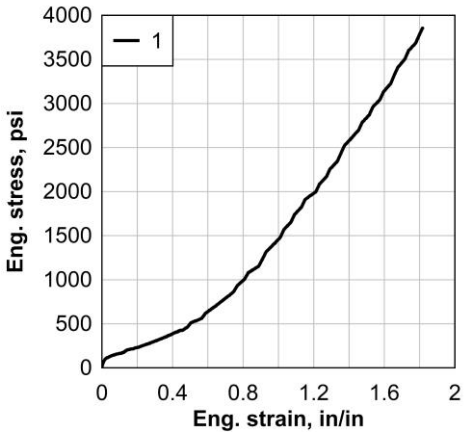

Figure 29: PVB In-Glass Static

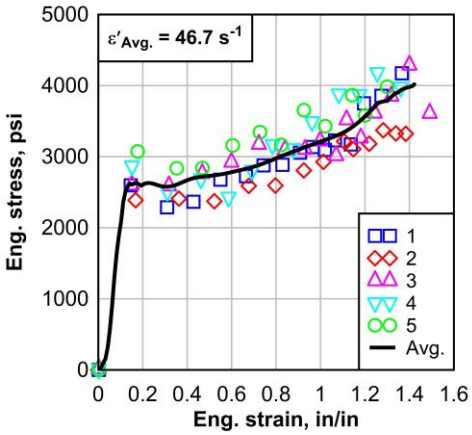

Figure 30: PVB Weathered Dynamic

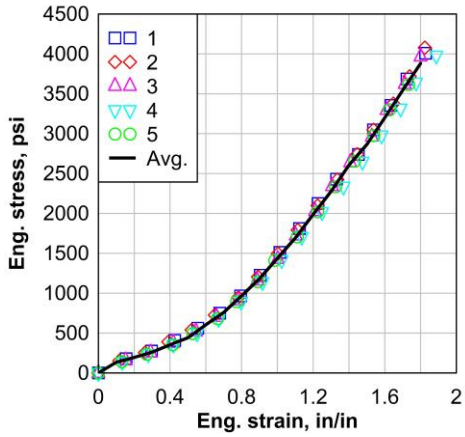

Figure 31: PVB Out-of-Glass Static

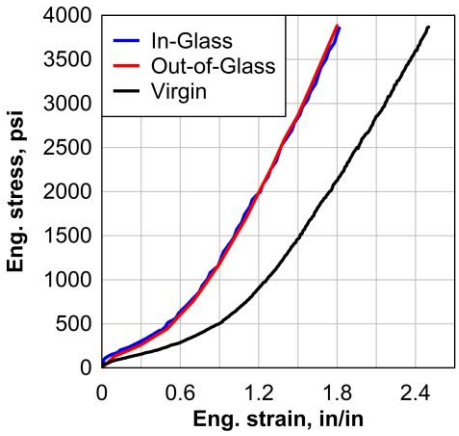

Figure 32: PVB Comparison Static

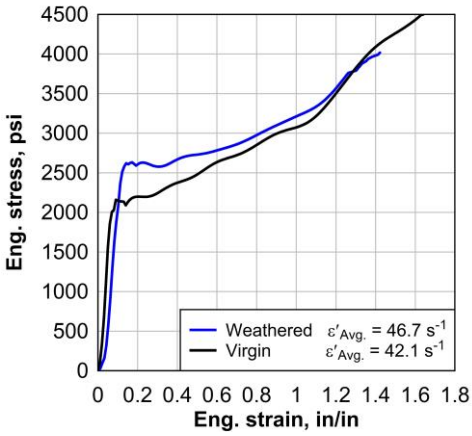

Figure 33: PVB Comparison Dynamic

Table 17: PVB Virgin Static Test Results

PVB Virgin							
No.	Specimen	Temperature, °F	Experimental Strain Rate, $\dot{\varepsilon}_E$ (s^{-1})	Failure Stress, σ_f (psi)	Failure Strain, ε_f (in/in)	Avg. Modulus, E_{avg} (psi)	Strain Energy, U (psi·in/in)
1	E-P-030-R-S-1	69	0.033	3741	2.626	1493	3511
2	E-P-030-R-S-2	69	0.033	3736	2.665	1481	3502
3	E-P-030-R-S-3	69	0.033	3821	2.782	1450	3598
4	E-P-030-R-S-4	69	0.033	3890	2.831	1407	3596
5	E-P-030-R-S-5	69	0.033	3255	2.550	1277	2730
Avg.		**69**	**0.033**	**3689**	**2.691**	**1422**	**3387**

Table 18: PVB In-Glass Static Test Results

PVB In-Glass							
No.	Specimen	Temperature, °F	Experimental Strain Rate, $\dot{\varepsilon}_E$ (s^{-1})	Failure Stress, σ_f (psi)	Failure Strain, ε_f (in/in)	Avg. Modulus, E_{avg} (psi)	Strain Energy, U (psi·in/in)
1	E-GP-030-R-033-1	66	0.033	3855	1.817	2165	2717
Avg.		**66**	**0.033**	**3855**	**1.817**	**2165**	**2717**

Table 19: PVB Out-of-Glass Static Test Results

PVB Out-of-Glass							
No.	Specimen	Temperature, °F	Experimental Strain Rate, $\dot{\varepsilon}_E$ (s^{-1})	Failure Stress, σ_f (psi)	Failure Strain, ε_f (in/in)	Avg. Modulus, E_{avg} (psi)	Strain Energy, U (psi·in/in)
1	E-WP-030-033-1	66	0.033	4072	1.841	2299	2862
2	E-WP-030-033-2	66	0.033	4196	1.847	2278	2907
3	E-WP-030-033-3	66	0.033	4033	1.826	2293	2768
4	E-WP-030-033-4	66	0.033	4027	1.907	2170	2906
5	E-WP-030-033-5	66	0.033	3928	1.808	2230	2658
Avg.		**66**	**0.033**	**4051**	**1.846**	**2254**	**2820**

Table 20: PVB Outdoor Weathering Static Test Results Comparison

PVB Static Comparison					
	Virgin	In-Glass	% Difference	Out-of-Glass	% Difference
Failure Stress, σ_f (psi)	3689	3855	4.51	4051	9.83
Failure Strain, ε_f (in/in)	2.691	1.817	-32.5	1.846	-31.4
Average Modulus, E_{avg} (psi)	1422	2165	52.3	2254	58.6
Strain Energy, U (psi·in/in)	3387	2717	-19.8	2820	-16.7

Table 21: PVB Virgin Dynamic Test Results

PVB Virgin										
No.	Specimen	Temperature, °F	Experimental Strain Rate, $\dot{\varepsilon}_E$ (s^{-1})	Pseudo-yield Stress, $\sigma_{ps,y}$	Pseudo-yield Strain, $\varepsilon_{ps,y}$	Failure Stress, σ_f (psi)	Failure Strain, ε_f (in/in)	Initial Modulus, E_{ini} (psi)	Secondary Modulus, E_{sec} (psi)	Strain Energy, U (psi·in/in)
1	E-P-030-R68-045-1	68	43.38	2585	0.124	4799	1.746	24,440	1592	5380
2	E-P-030-R68-045-2	68	42.36	2274	0.114	4340	1.651	24,007	1690	4665
3	E-P-030-R68-045-3	68	41.18	2163	0.085	4599	1.622	30,626	1607	4843
4	E-P-030-R68-045-4	68	41.54	2607	0.137	4729	1.650	20,041	1659	5069
5	E-P-030-R68-045-5	68	42.15	2036	0.070	4562	1.800	36,939	1687	5601
Avg.		**68**	**42.12**	**2333**	**0.106**	**4606**	**1.694**	**27,211**	**1647**	**5112**

Table 22: PVB Weathered Dynamic Test Results

PVB Weathered										
No.	Specimen	Temperature, °F	Experimental Strain Rate, $\dot{\varepsilon}_E$ (s^{-1})	Pseudo-yield Stress, $\sigma_{ps,y}$ (psi)	Pseudo-yield Strain, $\varepsilon_{ps,y}$ (in/in)	Failure Stress, σ_f (psi)	Failure Strain, ε_f (in/in)	Initial Modulus, E_{ini} (psi)	Secondary Modulus, E_{sec} (psi)	Strain Energy, U (psi·in/in)
1	WS-035-R-045	68	41.25	2596	0.146	4340	1.432	21,739	1494	3922
2	WS-035-R-045	68	45.04	2604	0.223	3506	1.480	14,705	1126	3828
3	WS-035-R-045	68	51.23	2695	0.122	4487	1.491	27,085	1140.0	4471
4	WS-035-R-045	68	49.07	2923	0.159	4491	1.423	21,598	1384	4358
5	WS-035-R-045	68	46.79	3088	0.185	3973	1.345	21,351	1217	4037
Avg.		**68**	**46.68**	**2781**	**0.167**	**4159**	**1.434**	**21,296**	**1272**	**4123**

Table 23: PVB Outdoor Weathering Dynamic Test Results Comparison

PVB Dynamic Comparison			
	Virgin	Weathered	% Difference
Experimental Strain Rate, $\dot{\varepsilon}_E$	42.12	46.68	10.81
Pseudo-yield Stress, $\sigma_{ps,y}$ (psi)	2333	2781	19.21
Pseudo-yield Strain, $\varepsilon_{ps,y}$ (in/in)	0.106	0.167	57.55
Failure Stress, σ_f (psi)	4606	4159	-9.69
Failure Strain, ε_f (in/in)	1.694	1.434	-15.33
Initial Modulus, E_{ini} (psi)	27211	21296	-21.74
Secondary Modulus, E_{sec} (psi)	1647	1272	-22.76
Strain Energy, U (psi·in/in)	5112	4123	-19.34

The results of the outdoor weathering one-month tests for Saflex Standard Clear PVB show a significant change in behavior after weathering. Figure 29 and Figure 31 show the quasi-static test results for PVB in-glass and out-of-glass respectfully. Samples from in-glass and

out-of-glass were mixed during cutting. Therefore, only one static sample was identified as in-glass and is presented in Figure 29. The dynamic specimens could not be distinguished as in-glass or out-of-glass; therefore, tests results shown in Figure 30 are for both and are termed “weathered” for the comparison to virgin PVB.

Figure 31 shows the stress-strain results of the five out-of-glass static tests as well as the average of those tests. There is not much variance between the five curves, showing that the static behavior of PVB is precise. It can be seen in Figure 32 that both the in-glass and out-of-glass PVB had improved performance. Because the weathered PVB achieved failure at a lower strain, the total strain energy is also lower, but the weathered PVB had a higher energy absorption up to a strain of 1.8 in/in. As discussed in the introduction, energy absorption is an important characteristic for blast-resistant design. Also notice that the average modulus of the curve increased by over 50% for both in-glass and out-of-glass PVB (Table 20). The weathering caused the materials to stiffen.

The dynamic test comparison also shows improved behavior for the weathered PVB. The pseudo-yield is 19% higher and the initial modulus is 22% higher. The strain energy is also 19% higher (Table 23). The weathered PVB was stiffer and absorbed more energy than the virgin material. The stiffness is expected as this property has been observed in previous natural weathering studies. In conclusion, the one-month weathered PVB showed improved performance in comparison to the virgin material.

Static

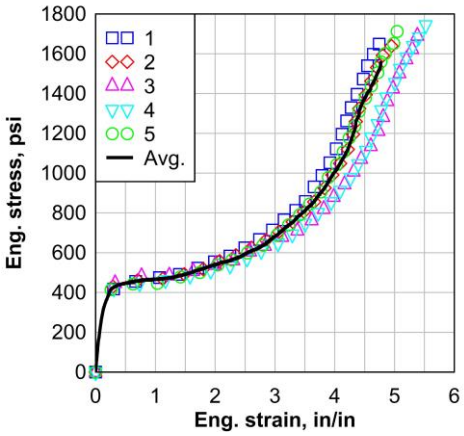

Figure 34:EVA In-Glass Static

Dynamic

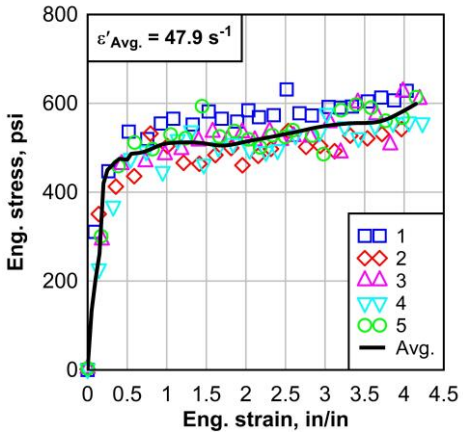

Figure 35: EVA In-Glass Dynamic

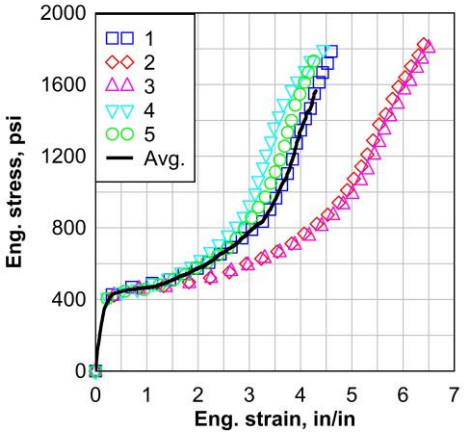

Figure 36: EVA Out-of-Glass Static

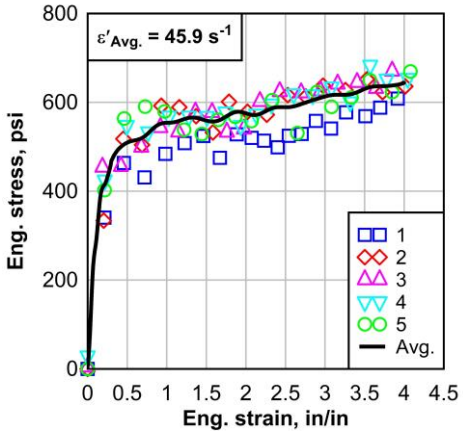

Figure 37: EVA Out-of-Glass Dynamic

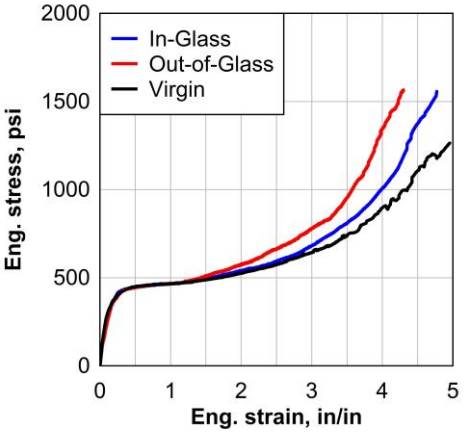

Figure 38: EVA Comparison Static

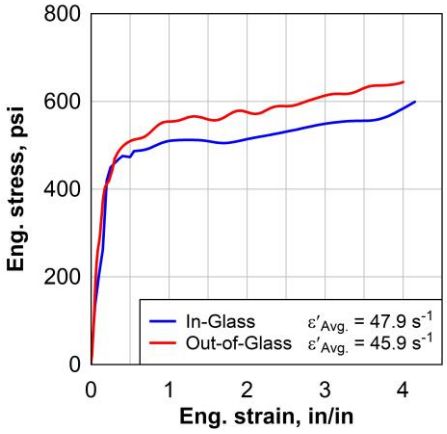

Figure 39: EVA Comparison Dynamic

Table 24: EVA Virgin Static Test Results

EVA Virgin (EVGuard)									
No.	Specimen	Temperature, °F	Experimental Strain Rate, $\dot{\varepsilon}_E$ (s^{-1})	Pseudo-yield Stress, $\sigma_{ps,y}$ (psi)	Pseudo-yield Strain, $\varepsilon_{ps,y}$ (in/in)	Failure Stress, σ_f (psi)	Failure Strain, ε_f (in/in)	Initial Modulus, E_{ini} (psi)	Strain Energy, U (psi·in/in)
1	S-E-030-R-033-1	66	0.033	449.6	0.454	1642	4.955	2245	3682
2	S-E-030-R-033-2	66	0.033	446.4	0.489	1770	6.426	2182	5149
3	S-E-030-R-033-3	66	0.033	452.8	0.452	1670	6.197	2018	4777
4	S-E-030-R-033-4	66	0.033	449.6	0.453	1868	6.149	2293	4982
5	S-E-030-R-033-5	66	0.033	440.0	0.485	2063	7.135	2552	6077
Avg.		**66**	**0.033**	**447.7**	**0.467**	**1803**	**6.172**	**2258**	**4933**

Table 25: EVA In-Glass Static Test Results

EVA In-Glass									
No.	Specimen	Temperature, °F	Experimental Strain Rate, $\dot{\varepsilon}_E$ (s^{-1})	Pseudo-yield Stress, $\sigma_{ps,y}$ (psi)	Pseudo-yield Strain, $\varepsilon_{ps,y}$ (in/in)	Failure Stress, σ_f (psi)	Failure Strain, ε_f (in/in)	Initial Modulus, E_{ini} (psi)	Strain Energy, U (psi·in/in)
1	S-GE-030-R-033-1	66	0.033	446.4	0.471	1655	4.771	2000	3499
2	S-GE-030-R-033-2	66	0.033	458.2	0.468	1651	4.932	2462	3584
3	S-GE-030-R-033-3	66	0.033	471.9	0.496	1709	5.443	2135	4081
4	S-GE-030-R-033-4	66	0.033	446.4	0.459	1766	5.549	2265	4211
5	S-GE-030-R-033-5	66	0.033	446.4	0.510	1744	5.082	2456	3816
Avg.		**66**	**0.033**	**453.9**	**0.481**	**1705**	**5.155**	**2264**	**3838**

Table 26: EVA Out-of-Glass Static Test Results

EVA Out-of-Glass									
No.	Specimen	Temperature, °F	Experimental Strain Rate, $\dot{\varepsilon}_E$ (s^{-1})	Pseudo-yield Stress, $\sigma_{ps,y}$ (psi)	Pseudo-yield Strain, $\varepsilon_{ps,y}$ (in/in)	Failure Stress, σ_f (psi)	Failure Strain, ε_f (in/in)	Initial Modulus, E_{ini} (psi)	Strain Energy, U (psi·in/in)
1	S-WE-030-R-033-1	66	0.033	459.1	0.497	1814	4.651	1989	3608
2	S-WE-030-R-033-2	66	0.033	443.8	0.467	1825	6.402	2057	4998
3	S-WE-030-R-033-3	66	0.033	446.4	0.492	1837	6.550	2167	5102
4	S-WE-030-R-033-4	66	0.033	443.2	0.466	1794	4.439	2431	3781
5	S-WE-030-R-033-5	66	0.033	446.4	0.472	1763	4.300	2418	3254
Avg.		**66**	**0.033**	**447.8**	**0.479**	**1807**	**5.268**	**2212**	**4149**

Table 27: EVA Outdoor Weathering Static Test Results Comparison

EVA Static Comparison					
	Virgin	In-Glass	% Difference	Out-of-Glass	% Difference
Pseudo-yield Stress, $\sigma_{ps,y}$ (psi)	447.7	453.9	1.38	447.8	0.02
Pseudo-yield Strain, $\varepsilon_{ps,y}$ (in/in)	0.467	0.481	3.04	0.479	2.61
Failure Stress, σ_f (psi)	1803	1705	-5.41	1807	0.22
Failure Strain, ε_f (in/in)	6.172	5.155	-16.5	5.268	-14.6
Initial Modulus, E_{ini} (psi)	2258	2264	0.25	2212	-2.02
Strain Energy, U (psi·in/in)	4933	3838	-22.2	4149	-15.9

Table 28: EVA In-Glass Dynamic Test Results

EVA In-Glass							
No.	Specimen	Temperature, °F	Experimental Strain Rate, $\dot{\varepsilon}_E$ (s^{-1})	Failure Stress, σ_f (psi)	Failure Strain, ε_f (in/in)	Initial Modulus, E_{ini} (psi)	Strain Energy, U
1	GS-035-R-04	68	47.86	670	4.174	2127	2329
2	GS-035-R-04	68	46.27	564	4.18	2126	2157
3	GS-035-R-04	68	48.92	588	4.008	2375	1926
4	GS-035-R-04	68	47.75	555	4.260	1192	2155
5	GS-035-R-04	68	48.47	577	4.337	1667	2149
Avg.		**68**	**47.85**	**591**	**4.192**	**1897**	**2143**

Table 29: EVA Out-of-Glass Dynamic Test Results

EVA Out-of-Glass							
No.	Specimen	Temperature, °F	Experimental Strain Rate, $\dot{\varepsilon}_E$ (s^{-1})	Failure Stress, σ_f (psi)	Failure Strain, ε_f (in/in)	Initial Modulus, E_{ini} (psi)	Strain Energy, U
1	WS-035-R-04	68	44.05	617	4.010	1894	2024
2	WS-035-R-04	68	47.03	688	4.205	2732	2364
3	WS-035-R-04	68	45.57	686	4.009	3175	2332
4	WS-035-R-04	68	46.77	631	4.204	2424	2422
5	WS-035-R-04	68	46.09	676	4.084	2375	2293
Avg.		**68**	**45.90**	**660**	**4.102**	**2520**	**2287**

Table 30: EVA Outdoor Weathering Dynamic Test Results Comparison

EVA Dynamic Comparison			
	In-Glass	Out-of-Glass	% Difference
Experimental Strain Rate, $\dot{\varepsilon}_E$ (s^{-1})	47.85	45.90	-4.08
Failure Stress, σ_f (psi)	590.8	659.6	11.65
Failure Strain, ε_f (in/in)	4.192	4.102	-2.13
Initial Modulus, E_{ini} (psi)	1897	2520	32.81
Strain Energy, U (psi·in/in)	2143	2287	6.71

The above figures and tables show the quasi-static and dynamic test results of Evguard EVA in-glass and out-of-glass in comparison to the virgin material. The figures each show five stress-strain curves and the average of these curves. Figure 36 has three tests that

closely match and two tests that appear to behave differently, achieving significantly higher failure strains. After carefully looking through the data, there is no apparent explanation for these phenomena. The tables show typical values used in mechanical behavior comparison. For EVA, the pseudo-yield point was taken as the maximum stress and corresponding strain achieved before a strain of 0.5 in/in. The initial modulus was taken as the slope of the linear regression of the curve up to a strain of 0.15 in/in. This is more representative than taking a linear regression all the way to the yield point, because the curve flattens out significantly before the selected yield.

The comparison of the EVA static test results shows some minor change in the weathered specimen performance in comparison to the virgin material (Figure 38). The failure stress has a maximum difference of 5.4%, and the initial modulus only changed by about 2%. The failure strain and strain energy decreased by about 15% for the weathered materials, indicating that the weathered material is less ductile (Table 27). The useable portion of the curve, however, is under a strain value of about 2 in/in (see Section 3.3.2). In this portion of the curve, there was almost no change between the virgin and weathered materials.

Unfortunately, no virgin material was tested dynamically for this type of EVA. The in-glass and out-of-glass samples behaved very similarly with a difference in strain energy of only 6.7% (Table 30). In the continuing work, virgin samples will be tested dynamically to compare with the weathered specimens.

Static **Dynamic**

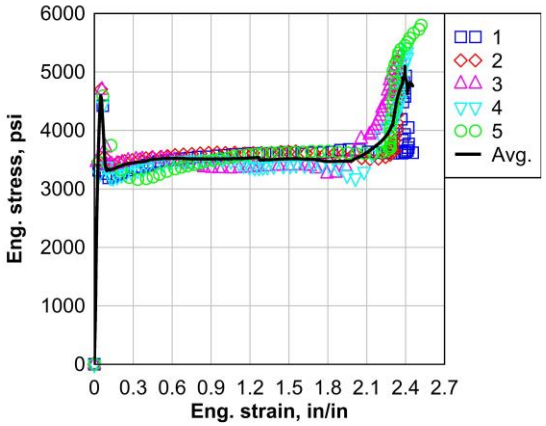

Figure 40: SG In-Glass Static

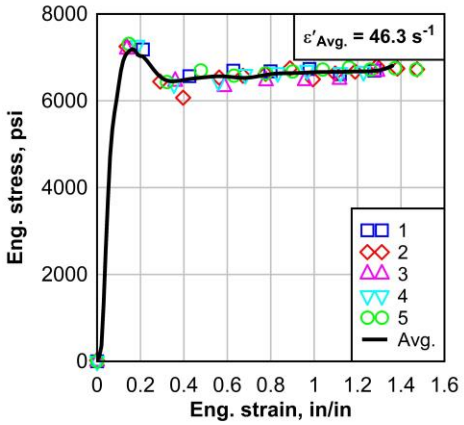

Figure 41: SG In-Glass Dynamic

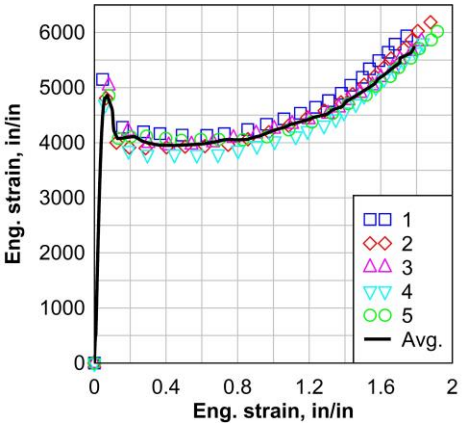

Figure 42: SG Out-of-Glass Static

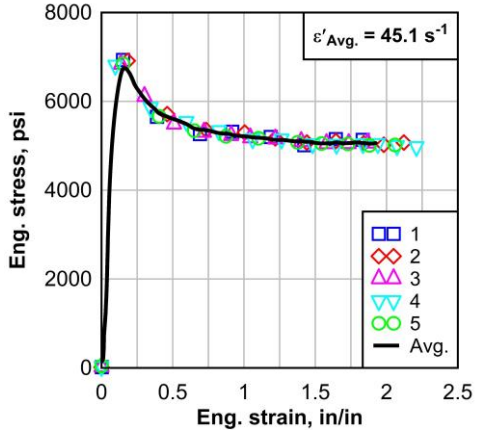

Figure 43: SG Out-of-Glass Dynamic

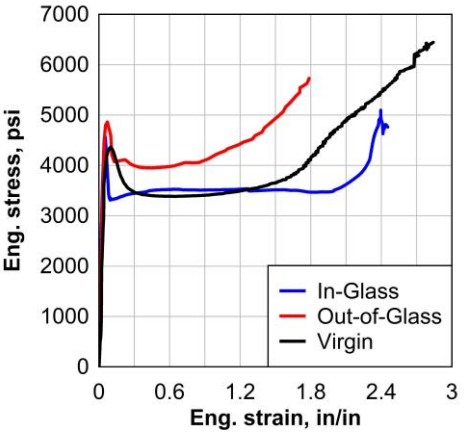

Figure 44: SG Comparison Static

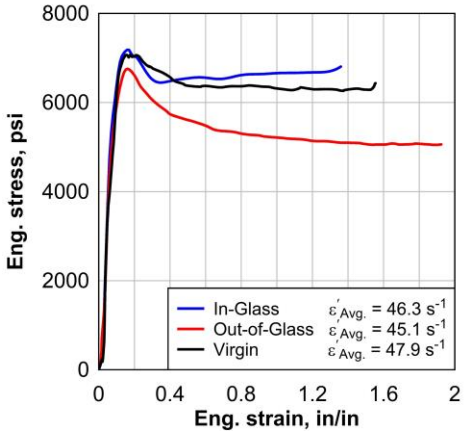

Figure 45: SG Comparison Dynamic

Table 31: SG Virgin Static Test Results

SG6000 Virgin										
No.	Specimen	Temperature, °F	Experimental Strain Rate, $\dot{\varepsilon}_E$ (s^{-1})	Pseudo-yield Stress, $\sigma_{ps,y}$ (psi)	Pseudo-yield Strain, $\varepsilon_{ps,y}$ (in/in)	Failure Stress, σ_f (psi)	Failure Strain, ε_f (in/in)	Initial Modulus, E_{ini} (psi)	Secondary Modulus, E_{sec} (psi)	Strain Energy, U (psi·in/in)
1	K-S6-035-R-033-1	66	0.033	4389	0.100	6516	2.801	47990	1160	11676
2	K-S6-035-R-033-2	66	0.033	4296	0.096	6520	2.726	49680	1170	11126
3	K-S6-035-R-033-3	66	0.033	4453	0.123	6726	2.946	47950	1187	12294
4	K-S6-035-R-033-4	66	0.033	4403	0.100	6669	2.980	54010	1143	12674
5	K-S6-035-R-033-5	66	0.033	4400	0.082	6300	2.813	66410	1094	11565
Avg.		**66**	**0.033**	**4388**	**0.100**	**6546**	**2.853**	**53208**	**1151**	**11867**

Table 32: SG In-Glass Static Test Results

SG In-Glass										
No.	Specimen	Temperature, °F	Experimental Strain Rate, $\dot{\varepsilon}_E$ (s^{-1})	Pseudo-yield Stress, $\sigma_{ps,y}$ (psi)	Pseudo-yield Strain, $\varepsilon_{ps,y}$ (in/in)	Failure Stress, σ_f (psi)	Failure Strain, ε_f (in/in)	Initial Modulus, E_{ini} (psi)	Secondary Modulus, E_{sec} (psi)	Strain Energy, U (psi·in/in)
1	K-GS-035-R-033-1	66	0.033	4517	0.058	5020	2.451	93290	333.1	8759
2	K-GS-035-R-033-2	66	0.033	4744	0.049	5234	2.321	104900	296.0	8239
3	K-GS-035-R-033-3	66	0.033	4720	0.051	5253	2.355	99730	468.3	8376
4	K-GS-035-R-033-4	66	0.033	4460	0.060	5422	2.412	83250	543.4	8375
5	K-GS-035-R-033-5	66	0.033	4646	0.059	5802	2.520	87700	685.1	9271
Avg.		**66**	**0.033**	**4617**	**0.055**	**5346**	**2.412**	**93774**	**465.2**	**8604**

Table 33: SG Out-of-Glass Static Test Results

SG Out-of-Glass										
No.	Specimen	Temperature, °F	Experimental Strain Rate, $\dot{\varepsilon}_E$ (s^{-1})	Pseudo-yield Stress, $\sigma_{ps,y}$ (psi)	Pseudo-yield Strain, $\varepsilon_{ps,y}$ (in/in)	Failure Stress, σ_f (psi)	Failure Strain, ε_f (in/in)	Initial Modulus, E_{ini} (psi)	Secondary Modulus, E_{sec} (psi)	Strain Energy, U (psi·in/in)
1	K-WS-035-R-033-1	66	0.033	5157	0.045	6067	1.786	125400	974.9	8193
2	K-WS-035-R-033-2	66	0.033	4818	0.060	6220	1.889	89690	1150	8404
3	K-WS-035-R-033-3	66	0.033	5045	0.076	5887	1.841	74250	927.0	8148
4	K-WS-035-R-033-4	66	0.033	4736	0.049	5930	1.894	102300	1093	8151
5	K-WS-035-R-033-5	66	0.033	4878	0.075	6130	1.943	73430	981.7	8664
Avg.		**66**	**0.033**	**4927**	**0.061**	**6047**	**1.871**	**93014**	**1025**	**8312**

Table 34: SG Outdoor Weathering Static Test Results Comparison

	SG Static Comparison				
	Virgin	In-Glass	% Difference	Out-of-Glass	% Difference
Pseudo-yield Stress, $\sigma_{ps,y}$ (psi)	5232	4617	-11.7	4927	-5.83
Pseudo-yield Strain, $\varepsilon_{ps,y}$ (in/in)	0.085	0.055	-34.6	0.061	-28.1
Failure Stress, σ_f (psi)	7322	5346	-27.0	6047	-17.4
Failure Strain, ε_f (in/in)	2.370	2.412	1.77	1.871	-21.1
Initial Modulus, E_{ini} (psi)	69716	93774	34.5	93014	33.4
Secondary Modulus, E_{sec} (psi)	1509	465.2	-69.2	1025	-32.1
Strain Energy, U (psi·in/in)	11526	8604	-25.4	8312	-27.9

Table 35: SG Virgin Dynamic Test Results

SG6000 Virgin										
No.	Specimen	Temperature, °F	Experimental Strain Rate, $\dot{\varepsilon}_E$ (s^{-1})	Pseudo-yield Stress, $\sigma_{ps,y}$ (psi)	Pseudo-yield Strain, $\varepsilon_{ps,y}$ (in/in)	Failure Stress, σ_f (psi)	Failure Strain, ε_f (in/in)	Initial Modulus, E_{ini} (psi)	Secondary Modulus, E_{sec} (psi)	Strain Energy, U (psi·in/in)
1	K-S6-035-R-045-1	68	45.78	7424	0.187	6474	1.555	48,382	-289	9740
2	K-S6-035-R-045-2	68	47.84	7357	0.148	6580	1.742	58,624	-267	10,964
3	K-S6-035-R-045-3	69	46.66	7173	0.105	5457	2.003	96,322	-461	11,392
4	K-S6-035-R-045-4	69	49.18	7140	0.117	6190	1.793	66,704	-273	10,973
5	K-S6-035-R-045-5	69	50.17	7248	0.208	6394	1.559	42,946	-314	9762
Avg.		**68.6**	**47.93**	**7268**	**0.153**	**6219**	**1.730**	**62,596**	**-321**	**10,566**

Table 36: SG In-Glass Dynamic Test Results

SG In-Glass										
No.	Specimen	Temperature, °F	Experimental Strain Rate, $\dot{\varepsilon}_E$ (s^{-1})	Pseudo-yield Stress, $\sigma_{ps,y}$ (psi)	Pseudo-yield Strain, $\varepsilon_{ps,y}$ (in/in)	Failure Stress, σ_f (psi)	Failure Strain, ε_f (in/in)	Initial Modulus, E_{ini} (psi)	Secondary Modulus, E_{sec} (psi)	Strain Energy, U (psi·in/in)
1	GS-035-R-045	69	47.13	7181	0.211	6561	1.362	43,777	1	8444
2	GS-035-R-045	69	42.84	7265	0.128	6857	1.504	68,935	171	9664
3	GS-035-R-045	69	48.34	7198	0.142	6680	1.291	59,939	-35	8199
4	GS-035-R-045	69	45.94	7278	0.186	6725	1.318	50,647	40	8291
5	GS-035-R-045	69	47.38	7310	0.146	6794	1.541	62,112	42	9990
Avg.		**69**	**46.33**	**7246**	**0.163**	**6723**	**1.403**	**57,082**	**43.8**	**8918**

Table 37: SG Out-of-Glass Dynamic Test Results

SG Out-of-Glass										
No.	Specimen	Temperature, °F	Experimental Strain Rate, $\dot{\varepsilon}_E$ (s^{-1})	Pseudo-yield Stress, $\sigma_{ps,y}$ (psi)	Pseudo-yield Strain, $\varepsilon_{ps,y}$ (in/in)	Failure Stress, σ_f (psi)	Failure Strain, ε_f (in/in)	Initial Modulus, E_{ini} (psi)	Secondary Modulus, E_{sec} (psi)	Strain Energy, U (psi·in/in)
1	WS-035-R-045	69	55.180	6934	0.145	4908	1.924	59,797	-595	10,287
2	WS-035-R-045	69	42.220	6914	0.184	5005	2.187	46,805	-514	11,461
3	WS-035-R-045	69	46.120	6845	0.144	5020	1.959	57,269	-625.0	10,340
4	WS-035-R-045	69	39.780	6814	0.101	5042	2.358	84,332	-494	12,342
5	WS-035-R-045	69	42.290	6847	0.150	4956	2.133	57,797	-576	11,089
Avg.		**69**	**45.12**	**6871**	**0.145**	**4986**	**2.112**	**61,200**	**-561**	**11,104**

Table 38: SG Outdoor Weathering Dynamic Test Results Comparison

SG Dynamic Comparison					
	Virgin	In-Glass	% Difference	Out-of-Glass	% Difference
Experimental Strain Rate, $\dot{\varepsilon}_E$ (s^{-1})	47.93	46.33	-3.34	45.12	-5.86
Pseudo-yield Stress, $\sigma_{ps,y}$ (psi)	7268	7246	-0.30	6871	-5.47
Pseudo-yield Strain, $\varepsilon_{ps,y}$ (in/in)	0.153	0.163	6.27	0.145	-5.36
Failure Stress, σ_f (psi)	6219	6723	8.11	4986	-19.82
Failure Strain, ε_f (in/in)	1.730	1.403	-18.91	2.112	22.06
Initial Modulus, E_{ini} (psi)	62596	57082	-8.81	61200	-2.23
Secondary Modulus, E_{sec} (psi)	-321	43.8	113.65	-561	-74.81
Strain Energy, U (psi·in/in)	10566	8918	-15.60	11104	5.09

The above figures show the quasi-static and dynamic test results of SG6000 in-glass and out-of-glass. The data is very clustered together because the behavior of the SG has little variance from sample to sample. Consistency is a good quality for any product, because the behavior is more predictable. The in-glass SG had a unique behavior during static testing. Near failure, the stress increased without a significant increase in strain. For the static tests, notice that the pseudo-yield stress and strain decreased, and the initial modulus increased by over 30% for both in-glass and out-of-glass. This means stiffening occurred as a result of the exposure. Notice also that the strain energy decreased by over 25% for both in-glass and out-of-glass. This means natural weathering could have a negative impact on the ability of SG to absorb energy in a blast scenario.

Investigating the dynamic behavior, Figure 45 seems to indicate that the in-glass and virgin materials behaved similarly, while the out-of-glass material behavior worsened. While the out-of-glass material had a decrease in pseudo-yield stress and failure stress, the strain energy increased by 5% indicating a possible improvement in material behavior. The cause of this increased strain energy is an increase in failure strain, meaning the out-of-glass material exhibited a higher ductility. Contrary to the static test results, the initial moduli for the dynamic in-glass and out-of-glass materials decreased slightly, so no stiffening effect was detected.

Table 39: Qualitative Summary of Outdoor Weathering One-Month Results

	Static		Dynamic	
	In-Glass	**Out-of-Glass**	**In-Glass**	**Out-of-Glass**
PVB	Improved	Improved	Improved*	
EVA	Improved	Improved	No Data	No Data
SG	No Change	Improved	No Change	Worsened
*No in-glass vs. out-of-glass				

In general, the outdoor weathering caused stiffening indicated by an increase in initial modulus for PVB and SG. This stiffening was not seen in EVA. A decrease in strain energy also appeared to be a common result of weathering for all three materials. It is difficult to draw a conclusion on whether the material was most affected in-glass or out-of-glass. Perhaps future testing at 3, 6, 9, and 12 months will show a clearer difference between the in-glass and out-of-glass behavior.

4.4 WATER IMMERSION RESULTS AND DISCUSSION

One of the main issues identified with the use of PVB is that it absorbs water if the LG window is not properly sealed around the frame. This could affect the mechanical and adhesion properties of the interlayer, as well as affect the optical characteristics. Because of this issue, EVA and SG have been marketed as hydrophobic, implying that the water damage to LG windows bonded with PVB will not occur in windows bonded with EVA and SG. The study in this section will compare the water absorption characteristics of Saflex Standard Clear PVB, SE-381TF EVA, and SG5000.

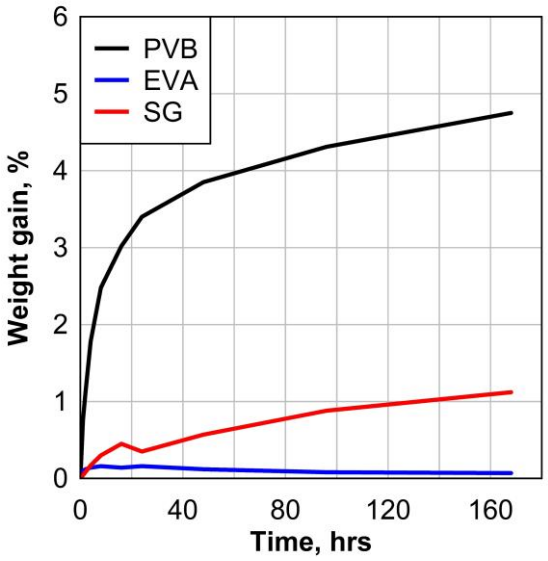

Figure 46: Weight Gain of Static Water Immersion Specimens Over Time

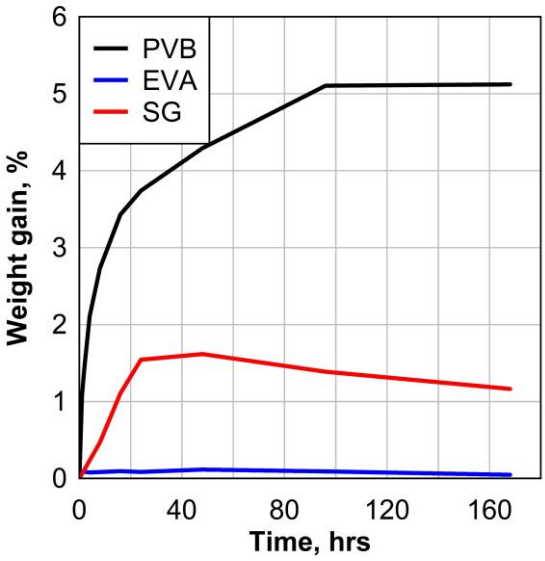

Figure 47: Weight Gain of Dynamic Water Immersion Specimens Over Time

As expected, the PVB had the greatest percentage of weight gain over time at about 5% over a period of 168 hours. The SG appears to have some weight gain of about 1%. Measures were taken to mitigate this effect on future weigh-ins. EVA had little to no weight gain, so this material is hydrophobic as advertised.

Static

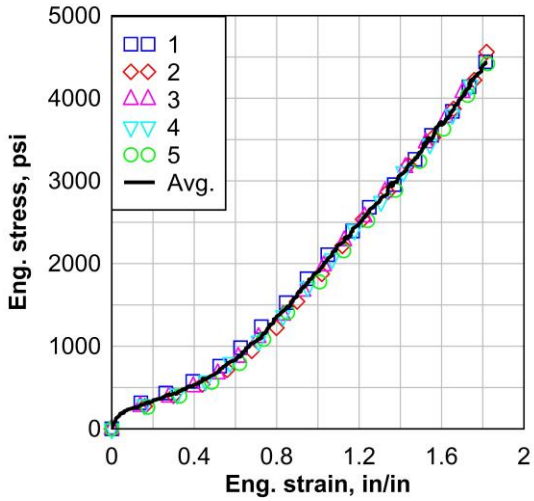

Figure 48: PVB Water Immersion Static

Dynamic

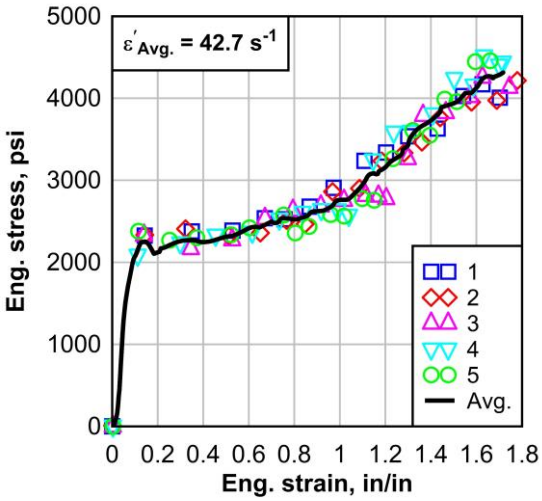

Figure 49: PVB Water Immersion Dynamic

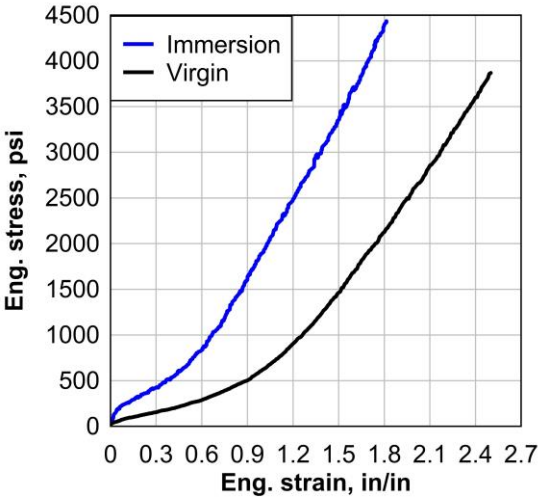

Figure 50: PVB Water Immersion Comparison Static

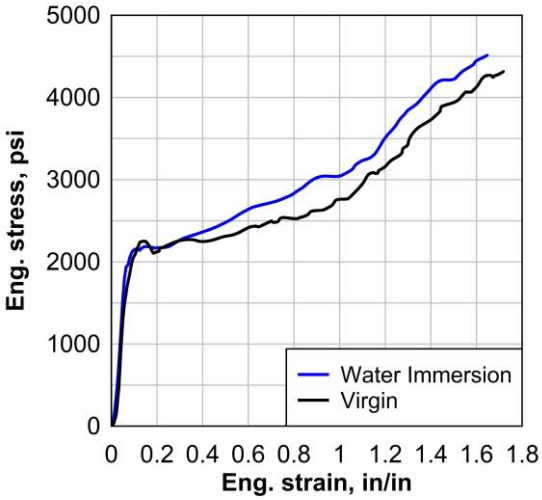

Figure 51: PVB Water Immersion Comparison Dynamic

Table 40: PVB Virgin Static Test Results

PVB Virgin							
No.	Specimen	Temperature, °F	Experimental Strain Rate, $\dot{\varepsilon}_E$ (s^{-1})	Failure Stress, σ_f (psi)	Failure Strain, ε_f (in/in)	Avg. Modulus, E_{avg} (psi)	Strain Energy, U (psi·in/in)
1	E-P-030-R-S-1	69	0.033	3741	2.626	1493	3511
2	E-P-030-R-S-2	69	0.033	3736	2.665	1481	3502
3	E-P-030-R-S-3	69	0.033	3821	2.782	1450	3598
4	E-P-030-R-S-4	69	0.033	3890	2.831	1407	3596
5	E-P-030-R-S-5	69	0.033	3255	2.550	1277	2730
Avg.		**69**	**0.033**	**3689**	**2.691**	**1422**	**3387**

Table 41: PVB Water Immersion Static Test Results

PVB Water Immersion							
No.	Specimen	Temperature, °F	Experimental Strain Rate, $\dot{\varepsilon}_E$ (s^{-1})	Failure Stress, σ_f (psi)	Failure Strain, ε_f (in/in)	Avg. Modulus, E_{avg} (psi)	Strain Energy, U (psi·in/in)
1	E-IP-030-R-033-1	66	0.033	4457	1.814	2469	3406
2	E-IP-030-R-033-2	66	0.033	4589	1.855	2552	3447
3	E-IP-030-R-033-3	66	0.033	4378	1.781	2524	3203
4	E-IP-030-R-033-4	66	0.033	4263	1.781	2461	3149
5	E-IP-030-R-033-5	66	0.033	4451	1.843	2488	3300
Avg.		**66**	**0.033**	**4428**	**1.815**	**2499**	**3301**

Table 42: PVB Water Immersion Static Test Results Comparison

PVB Static Comparison			
	Virgin	Immersed	% Difference
Failure Stress, σ_f (psi)	3689	4428	20.0
Failure Strain, ε_f (in/in)	2.691	1.815	-32.6
Avg. Modulus, E_{avg} (psi)	1422	2499	75.8
Strain Energy, U (psi·in/in)	3387	3301	-2.55

Table 43: PVB Virgin Dynamic Test Results

PVB Virgin										
No.	Specimen	Temperature, °F	Experimental Strain Rate, $\dot{\varepsilon_E}$ (s^{-1})	Pseudo-yield Stress, $\sigma_{ps,y}$ (psi)	Pseudo-yield Strain, $\varepsilon_{ps,y}$ (in/in)	Failure Stress, σ_f (psi)	Failure Strain, ε_f (in/in)	Initial Modulus, E_{ini} (psi)	Secondary Modulus, E_{sec} (psi)	Strain Energy, U (psi·in/in)
1	E-P-030-R68-045-1	68	43.38	2585	0.124	4799	1.746	24,440	1592	5380
2	E-P-030-R68-045-2	68	42.36	2274	0.114	4340	1.651	24,007	1690	4665
3	E-P-030-R68-045-3	68	41.18	2163	0.085	4599	1.622	30,626	1607	4843
4	E-P-030-R68-045-4	68	41.54	2607	0.137	4729	1.650	20,041	1659	5069
5	E-P-030-R68-045-5	68	42.15	2036	0.070	4562	1.800	36,939	1687	5601
Avg.		**68**	**42.12**	**2333**	**0.106**	**4606**	**1.694**	**27,211**	**1647**	**5112**

Table 44: PVB Water Immersion Dynamic Test Results

PVB Water Immersion										
No.	Specimen	Temperature, °F	Experimental Strain Rate, $\dot{\varepsilon_E}$ (s^{-1})	Pseudo-yield Stress, $\sigma_{ps,y}$ (psi)	Pseudo-yield Strain, $\varepsilon_{ps,y}$ (in/in)	Failure Stress, σ_f (psi)	Failure Strain, ε_f (in/in)	Initial Modulus, E_{ini} (psi)	Secondary Modulus, E_{sec} (psi)	Strain Energy, U (psi·in/in)
1	E-IP-030-R-045-1	68	41.82	2326	0.143	4062	1.717	19,796	1455	4880
2	E-IP-030-R-045-2	68	44.31	2335	0.143	4109	1.795	17,890	1487	5077
3	E-IP-030-R-045-3	68	43.10	2336	0.148	4742	1.774	17,199	1559	5028
4	E-IP-030-R-045-4	68	40.33	2088	0.112	4011	1.792	23,946	1758	5243
5	E-IP-030-R-045-5	68	43.91	2380	0.115	4574	1.665	25,030	1600	4483
Avg.		**68**	**42.69**	**2293**	**0.132**	**4300**	**1.749**	**20,772**	**1571.8**	**4942**

Table 45: PVB Water Immersion Dynamic Test Results Comparison

PVB Dynamic Comparison			
	Virgin	Water Immersion	% Difference
Pseudo-yield Stress, $\sigma_{ps,y}$ (psi)	2333	2293	-1.71
Pseudo-yield Strain, $\varepsilon_{ps,y}$ (in/in)	0.106	0.132	24.7
Failure Stress, σ_f (psi)	4606	4300	-6.65
Failure Strain, ε_f (in/in)	1.694	1.749	3.24
Initial Modulus, E_{ini} (psi)	27,211	20,772	-23.7
Secondary Modulus, E_{sec} (psi)	1647	1571.8	-4.57
Strain Energy, U (psi·in/in)	5112	4942	-3.31

The PVB absorbed the most water according to Figure 46 and Figure 47. The static results show a dramatic stiffening effect; Table 42 shows a 75% increase in average strain. The dynamic test results, however, show a 24% decrease in initial modulus meaning the immersed material was less stiff. The strain energy for both static and dynamic showed very little change. While Figure 50 shows a clear difference in static behavior between the

virgin and water immersion materials, Figure 51 shows a lot of similarity in the dynamic behavior. Thus, no clear conclusion can be drawn.

It is also important to note that the PVB specimens became opaquer in the water, turning a milky white color instead of their typical clear (Figure 53). This opaqueness disappeared after drying the specimen in the oven at the end of the 168-hour weighing period (Figure 52). This change could cause visibility issues for LG windows bonded with PVB.

Figure 52:Immersed PVB Dynamic Specimens After Testing

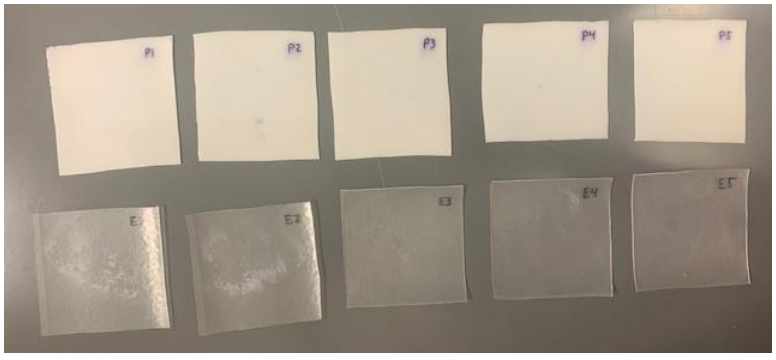

Figure 53: Immersed PVB versus EVA Visual Comparison

Static **Dynamic**

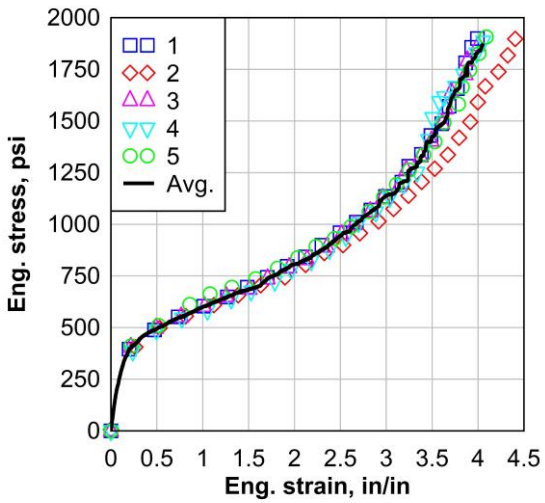

Figure 54: EVA Water Immersion Static

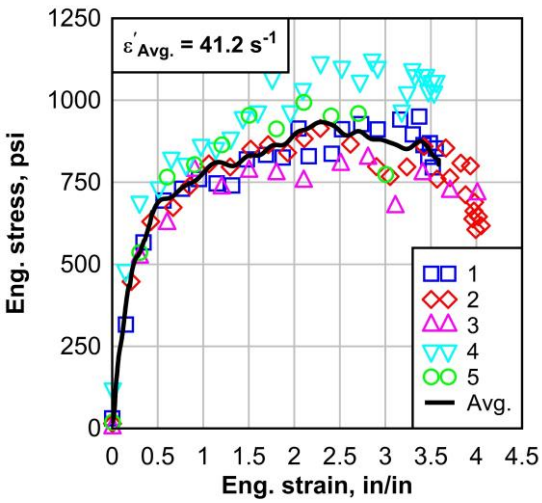

Figure 55:EVA Water Immersion Dynamic

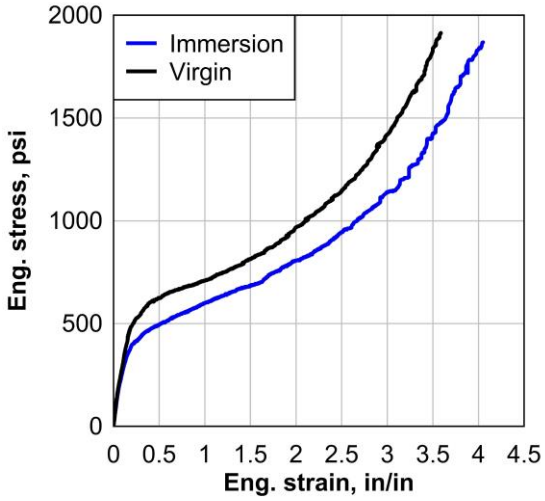

Figure 56: EVA Water Immersion Comparison Static

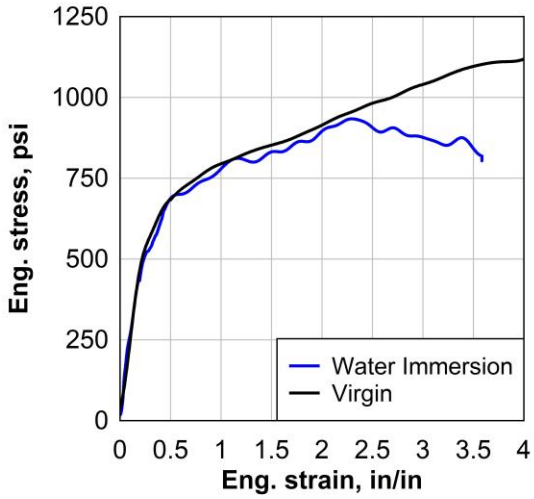

Figure 57: EVA Water Immersion Comparison Dynamic

Table 46: EVA Virgin Static Test Results

EVA Virgin (SE-381TF)									
No.	Specimen	Temperature, °F	Experimental Strain Rate, $\dot{\varepsilon}_E$ (s^{-1})	Pseudo-yield Stress, $\sigma_{ps,y}$ (psi)	Pseudo-yield Strain, $\varepsilon_{ps,y}$ (in/in)	Failure Stress, σ_f (psi)	Failure Strain, ε_f (in/in)	Initial Modulus, E_{ini} (psi)	Strain Energy, U (psi·in/in)
1	W-E-030-R-033-1	66	0.033	640.9	0.491	1954	3.589	2769	3587
2	W-E-030-R-033-2	66	0.033	612.2	0.496	1935	3.649	2659	3566
3	W-E-030-R-033-3	66	0.033	619.5	0.487	2025	3.725	2644	3727
4	W-E-030-R-033-4	66	0.033	631.3	0.486	2209	4.012	2911	4379
5	W-E-030-R-033-5	66	0.033	612.2	0.491	2018	4.024	2804	4066
Avg.		**66**	**0.033**	**623.2**	**0.490**	**2028**	**3.800**	**2757**	**3865**

Table 47: EVA Water Immersion Static Test Results

EVA Water Immersion									
No.	Specimen	Temperature, °F	Experimental Strain Rate, $\dot{\varepsilon}_E$ (s^{-1})	Pseudo-yield Stress, $\sigma_{ps,y}$ (psi)	Pseudo-yield Strain, $\varepsilon_{ps,y}$ (in/in)	Failure Stress, σ_f (psi)	Failure Strain, ε_f (in/in)	Initial Modulus, E_{ini} (psi)	Strain Energy, U (psi·in/in)
1	S-IE-030-R-033-1	66	0.033	494.8	0.491	1916	4.051	2069	3688
2	S-IE-030-R-033-2	66	0.033	487.8	0.492	1888	4.439	2282	4066
3	S-IE-030-R-033-3	66	0.033	500.6	0.496	1939	4.375	2136	4274
4	S-IE-030-R-033-4	66	0.033	487.8	0.478	1933	4.134	2045	3257
5	S-IE-030-R-033-5	66	0.033	507.0	0.492	1891	4.146	2402	3871
Avg.		**66**	**0.033**	**495.6**	**0.490**	**1913**	**4.229**	**2187**	**3831**

Table 48: EVA Water Immersion Static Test Results Comparison

EVA Static Comparison			
	Virgin	Immersed	% Difference
Pseudo-yield Stress, $\sigma_{ps,y}$ (psi)	623	495.6	-20.48
Pseudo-yield Strain, $\varepsilon_{ps,y}$ (in/in)	0.490	0.490	-0.08
Failure Stress, σ_f (psi)	2028	1913	-5.66
Failure Strain, ε_f (in/in)	3.800	4.229	11.3
Initial Modulus, E_{ini} (psi)	2757	2187	-20.69
Strain Energy, U (psi·in/in)	3865	3831	-0.9

Table 49: EVA Virgin Dynamic Test Results

EVA Virgin (SE-381TF)							
No.	Specimen	Temperature, °F	Experimental Strain Rate, $\dot{\varepsilon}_E$ (s^{-1})	Failure Stress, σ_f (psi)	Failure Strain, ε_f (in/in)	Initial Modulus, E_{ini} (psi)	Strain Energy, U (psi·in/in)
1	W-E-030-R-033-1	66	46.53	1047	4.033	4012	3608
2	W-E-030-R-033-2	66	45.31	1225	4.400	3078	3677
3	W-E-030-R-033-3	66	44.97	1101	3.974	2640	3510
4	W-E-030-R-033-4	66	44.28	1269	4.285	3229	3898
5	W-E-030-R-033-5	66	44.77	1037	4.289	2251	3911
Avg.		**66**	**45.17**	**1136**	**4.196**	**3042**	**3721**

Table 50: EVA Water Immersion Dynamic Test Results

EVA Water Immersion							
No.	Specimen	Temperature, °F	Experimental Strain Rate, $\dot{\varepsilon}_E$ (s^{-1})	Failure Stress, σ_f (psi)	Failure Strain, ε_f (in/in)	Initial Modulus, E_{ini} (psi)	Strain Energy, U (psi·in/in)
1	S-IE-030-R-045-1	68	40.71	699	3.585	1999	2785
2	S-IE-030-R-045-2	68	41.42	611	4.055	2904	3089
3	S-IE-030-R-045-3	68	40.61	682	4.114	2574	2918
4	S-IE-030-R-045-4	68	41.07	1103	3.573	2565	3376
5	S-IE-030-R-045-5	68	42.34	797	3.249	2458	2680
Avg.		**68**	**41.23**	**778**	**3.715**	**2500**	**2970**

Table 51: EVA Water Immersion Dynamic Test Results Comparison

EVA Dynamic Comparison			
	Virgin	Water Immersion	% Difference
Failure Stress, σ_f (psi)	1136	778	-31.5
Failure Strain, ε_f (in/in)	4.196	3.715	-11.5
Initial Modulus, E_{ini} (psi)	3042	2500	-17.8
Strain Energy, U (psi·in/in)	3721	2970	-20.2

Although the EVA did not absorb water, the static and dynamic behavior both worsened. This is apparent in the 20% decrease in both pseudo-yield stress and strain energy for the static test (Table 48). Also, the dynamic test had a 31.5% decrease in failure stress and a 20% decrease in strain energy (Table 51). There was clearly damage to the EVA due to the water immersion process, even though the material was hydrophobic. Perhaps this

worsening behavior is a result of the oven drying. In this case, future environmental and temperature testing will reveal a worsening behavior at higher temperatures for EVA.

Visually, the EVA maintained its transparency, unlike PVB (Figure 53). This is beneficial for visibility should humidity enter the window frame.

Figure 58: Immersed EVA Dynamic Specimens After Testing

Static **Dynamic**

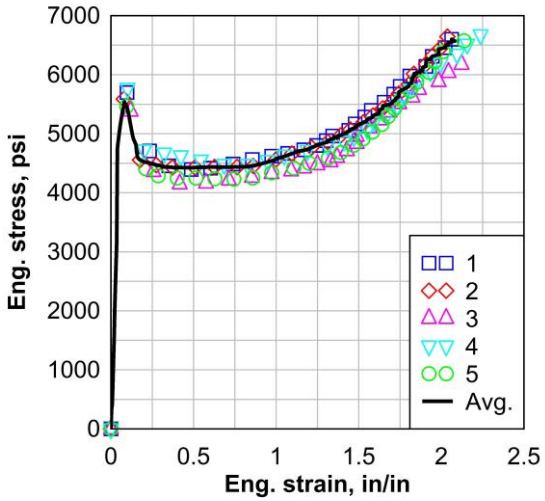

Figure 59: SG Water Immersion Static

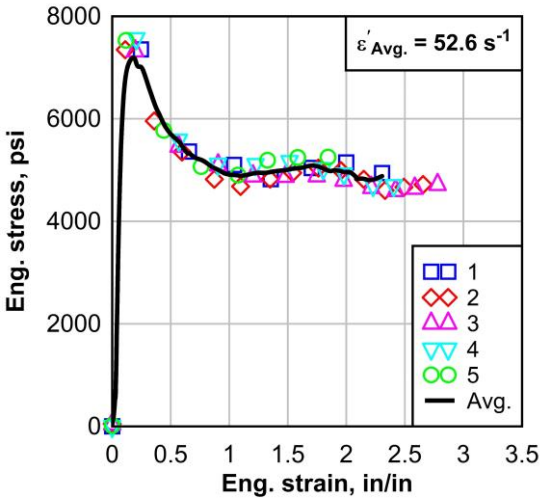

Figure 60: SG Water Immersion Dynamic

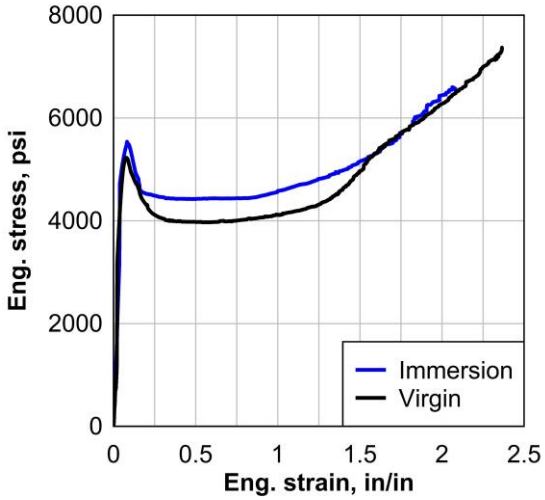

Figure 61: SG Water Immersion Comparison Static

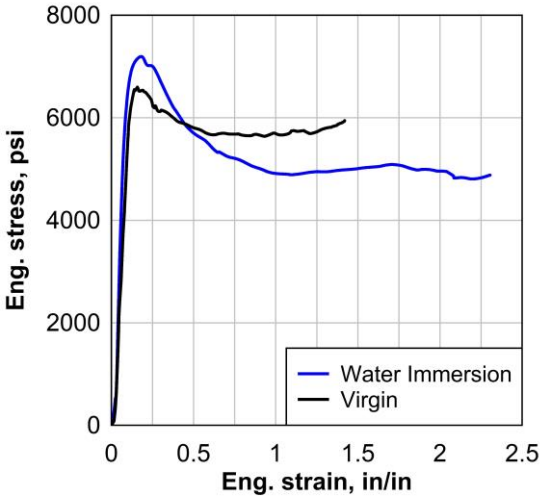

Figure 62: SG Water Immersion Comparison Dynamic

Table 52: SG Virgin Static Test Results

SG5000 Virgin										
No.	Specimen	Temperature, °F	Experimental Strain Rate, $\dot{\varepsilon}_E$ (s^{-1})	Pseudo-yield Stress, $\sigma_{ps,y}$ (psi)	Pseudo-yield Strain, $\varepsilon_{ps,y}$ (in/in)	Failure Stress, σ_f (psi)	Failure Strain, ε_f (in/in)	Initial Modulus, E_{ini} (psi)	Secondary Modulus, E_{sec} (psi)	Strain Energy, U (psi·in/in)
1	K-S5-035-R-033-1	66	0.033	5231	0.075	7384	2.365	77150	1549	11530
2	K-S5-035-R-033-2	66	0.033	5302	0.077	7286	2.318	75500	1465	11340
3	K-S5-035-R-033-3	66	0.033	5242	0.118	7229	2.362	44970	1525	11448
4	K-S5-035-R-033-4	66	0.033	5239	0.078	7603	2.419	76890	1618	11880
5	K-S5-035-R-033-5	66	0.033	5146	0.076	7106	2.385	74070	1388	11433
Avg.		**66**	**0.033**	**5232**	**0.085**	**7322**	**2.370**	**69716**	**1509**	**11526**

Table 53: SG Water Immersion Static Test Results

SG Water Immersion										
No.	Specimen	Temperature, °F	Experimental Strain Rate, $\dot{\varepsilon}_E$ (s^{-1})	Pseudo-yield Stress, $\sigma_{ps,y}$ (psi)	Pseudo-yield Strain, $\varepsilon_{ps,y}$ (in/in)	Failure Stress, σ_f (psi)	Failure Strain, ε_f (in/in)	Initial Modulus, E_{ini} (psi)	Secondary Modulus, E_{sec} (psi)	Strain Energy, U (psi·in/in)
1	K-IS-035-R-033-1	66	0.033	5703	0.090	6599	2.062	88360	984.0	10195
2	K-IS-035-R-033-2	66	0.033	5586	0.078	6701	2.076	62720	1024.0	10241
3	K-IS-035-R-033-3	66	0.033	5441	0.099	6308	2.182	69620	983.0	10326
4	K-IS-035-R-033-4	66	0.033	5769	0.101	6789	2.238	65130	918.4	11198
5	K-IS-035-R-033-5	66	0.033	5504	0.086	6575	2.137	71040	987.2	10216
Avg.		**66**	**0.033**	**5601**	**0.091**	**6594**	**2.139**	**71374**	**979.3**	**10435**

Table 54: SG Water Immersion Static Test Results Comparison

SG Static Comparison			
	Virgin	Immersed	% Difference
Pseudo-yield Stress, $\sigma_{ps,y}$ (psi)	5232	5601	7.0
Pseudo-yield Strain, $\varepsilon_{ps,y}$ (in/in)	0.085	0.091	7.0
Failure Stress, σ_f (psi)	7322	6594	-9.9
Failure Strain, ε_f (in/in)	2.370	2.139	-9.74
Initial Modulus, E_{ini} (psi)	69716	71374	2.4
Secondary Modulus, E_{sec} (psi)	1509	979.3	-35.1
Strain Energy, U (psi·in/in)	11526	10435	-9.5

Table 55: SG Virgin Dynamic Test Results

SG5000 Virgin										
No.	Specimen	Temperature, °F	Experimental Strain	Pseudo-yield Stress,	Pseudo-yield Strain,	Failure Stress, σ_f (psi)	Failure Strain, ε_f (in/in)	Initial Modulus, E_{ini} (psi)	Secondary Modulus, E_{sec} (psi)	Strain Energy, U (psi·in/in)
1	K-S5-035-R-045-1	68	38.96	6777	0.149	5757	1.544	75,761	-202	8885
2	K-S5-035-R-045-2	68	44.94	6918	0.172	5850	1.187	63,167	-573	6832
3	K-S5-035-R-045-3	68	50.21	6551	0.145	5030	1.153	56,275	-1177	5984
4	K-S5-035-R-045-4	68	40.13	6383	0.187	5687	1.437	46,349	-411	7826
5	K-S5-035-R-045-5	68	41.48	6642	0.134	5701	1.436	69,830	-421	8093
Avg.		**68**	**43.14**	**6654**	**0.157**	**5605**	**1.351**	**62,276**	**-557**	**7524**

Table 56: SG Water Immersion Dynamic Test Results

SG Water Immersion										
No.	Specimen	Temperature, °F	Experimental Strain Rate, $\dot{\varepsilon}_E$ (s^{-1})	Pseudo-yield Stress, $\sigma_{ps,y}$ (psi)	Pseudo-yield Strain, $\varepsilon_{ps,y}$ (in/in)	Failure Stress, σ_f (psi)	Failure Strain, ε_f (in/in)	Initial Modulus, E_{ini} (psi)	Secondary Modulus, E_{sec} (psi)	Strain Energy, U (psi·in/in)
1	K-IS-035-R-045-1	68	58.86	7373	0.251	4942	2.305	35,220	-657	11,765
2	K-IS-035-R-045-2	68	56.55	7349	0.112	4640	2.659	81,476	-527	13,536
3	K-IS-035-R-045-3	68	46.48	7324	0.196	4760	3.005	48,212	-452	15,021
4	K-IS-035-R-045-4	68	46.09	7583	0.230	4696	2.500	40,694	-680	13,227
5	K-IS-035-R-045-5	68	54.77	7544	0.124	5226	2.007	79,457	-778	10,728
Avg.		**68**	**52.55**	**7435**	**0.183**	**4853**	**2.495**	**57,012**	**-619**	**12,855**

Table 57: SG Water Immersion Dynamic Test Results Comparison

SG Dynamic Comparison			
	Virgin	Water Immersion	% Difference
Pseudo-yield Stress, $\sigma_{ps,y}$ (psi)	6654	7435	11.7
Pseudo-yield Strain, $\varepsilon_{ps,y}$ (in/in)	0.157	0.183	16.0
Failure Stress, σ_f (psi)	5605	4853	-13.4
Failure Strain, ε_f (in/in)	1.351	2.495	84.6
Initial Modulus, E_{ini} (psi)	62,276	57,012	-8.45
Secondary Modulus, E_{sec} (psi)	-557	-619	11.1
Strain Energy, U (psi·in/in)	7524	12,855	70.9

The SG did not have very significant weight gain during the water immersion process. The static test results show a small 7% increase in pseudo-yield stress and strain and about a 10% decrease in failure stress and strain. The strain energy also decreased by 9.5% (Table 54). The static test results do not show much change in mechanical behavior after water

immersion. The dynamic results, however, show a significant increase in ductility. The immersed SG achieved 84.6% higher failure strain, as well as 70.9% higher strain energy. The pseudo-yield stress and strain also increased (Table 57). The SG clearly performed better than the PVB and EVA after water immersion, thus making it the best candidate for resisting damage due to humidity.

The SG also remained transparent throughout the water immersion process, so visibility would not be an issue relating to humidity. Another important note is that two of the SG dynamic samples broke outside of the gage length. These are labeled in Figure 63 as S2 and S6. Both samples broke right where the tapered part of the specimen ends and the aluminum tab begins. This type of brittle failure did not occur with virgin materials. This shows that SG must have some unpredictable degradation due to the weathering.

Figure 63: Immersed SG Dynamic Specimens After Testing

5 CONCLUSIONS, RECOMMENDATIONS, AND FUTURE WORK

5.1 CONCLUSIONS

Chapter 3 investigated the effects of varying quasi-static strain rates on the mechanical behavior of PVB, EVA, and SG. The strain rate study showed that for PVB and SG, stiffening occurred with an increase in strain rate. This stiffening was most prominent for SG. EVA did not have a consistent stiffening. The strain energy was relatively similar regardless of strain rate with SG achieving the highest strain energy. In comparison to the dynamic strain rate, however, the PVB strain energy increased, the SG5000 strain energy decreased, and the SG6000 strain energy remained about the same at a strain rate of 45 s^{-1}.

Chapter 4 investigated the effects of outdoor weathering and water immersion on the mechanical behavior of PVB, EVA, and SG. The outdoor weathering caused stiffening in the SG and PVB that was not apparent in the EVA. All three materials showed a general decrease in strain energy as a result of weathering. A conclusion cannot yet be drawn on whether the material was most affected in-glass or out-of-glass because the affects vary significantly. The water immersion caused a 5% weight gain for the PVB, 1% for SG and 0% for EVA. The SG mechanical behavior improved significantly after water immersion with a drastic increase in failure strain leading to an increase in strain energy. The PVB had some inconsistent behavior with the static tests showing a stiffening and the dynamic tests showing a softening. Though the EVA had no water absorption, the mechanical behavior worsened. The EVA had softening and a decrease in strain energy for both static and dynamic testing.

Combined weathering of PVB and SG in general cause the material to stiffen, achieving higher stress but lower strain. EVA did not stiffen, and in fact showed some softening behavior overall.

5.2 RECOMMENDATIONS

For the strain rate study, it is recommended that the range of strain rates between the quasi-static and dynamic rates be tested. The strain rates between 1 s^{-1} and 45 s^{-1} could provide good insight on the transition of behavior between low and high strain rates. The outdoor weathering study is expected to continue for a full year, so no additional recommendations will be made at this time. For the water immersion study, it is recommended to perform water immersion of laminated glass discs for bond testing. This recommendation comes from the literature review, where several scholars noted that humidity has a greater effect on bond adhesion than on the polymer interlayer itself. Finally, as an overall recommendation, it would be beneficial to run all tests on the same material from the same manufacturer because the material behavior varies drastically between manufacturers. This is particularly noticeable for the Evguard EVA versus the SE-381TF EVA, one of which is used for outdoor weathering and the other for water immersion. A complete study could be done on the difference in behavior between the various manufacturers.

5.3 FUTURE WORK

Research continues at the University of Missouri-Columbia National Center for Explosion Resistant Design. The outdoor weathering specimens remain for a period of twelve months, and samples will be removed and tested every three months. The instruments measuring

temperature, precipitation, and solar radiation will be useful in describing the full scope of conditions experienced by the outdoor weathering specimens. Conclusions will be drawn on the difference in effect on interlayers in-glass versus out-of-glass.

From literature review, the effects of water immersion on bond adhesion are important to investigate. Thus, a bond test has been developed and small circular laminated glass samples are being prepared for conditioning following the water immersion procedure outlined in this study. Comparison will be made between the effects of water immersion on mechanical properties of the interlayer versus bond adhesion characteristics.

In addition to these continuations of the studies investigated herein, additional environmental impact studies will be conducted using an environmental chamber. This will allow for controlled temperature and humidity testing.

6 REFERENCES

Andreozzi, L., Briccoli Bati, S., Fagone, M., Ranocchiai, G., & Zulli, F. (2015). Weathering action on thermo-viscoelastic properties of polymer interlayers for laminated glass. *Construction and Building Materials*, *98*. https://doi.org/10.1016/j.conbuildmat.2015.08.010

Antolinc, D. (2020). Three-point bending test of laminated glass with PVB and EVA interlayers at elevated temperature.

ASTM International. D638-10 Standard Test Method for Tensile Properties of Plastics. West Conshohocken, PA, 2010, DOI: 10.1520/D0638-10, www.astm.org.

ASTM D570-98(2018), Standard Test Method for Water Absorption of Plastics, ASTM International, West Conshohocken, PA, 2018, DOI: 10.1520/D0570-98R18, www.astm.org.

ASTM D1435-13, Standard Practice for Outdoor Weathering of Plastics, ASTM International, West Conshohocken, PA, 2013, DOI: 10.1520/D1435-13, www.astm.org.

ASTM G7 / G7M-13, Standard Practice for Atmospheric Environmental Exposure Testing of Nonmetallic Materials, ASTM International, West Conshohocken, PA, 2013, DOI: 10.1520/G0007_G0007M-13, www.astm.org.

Bedon, C. (2019). Issues on the vibration analysis of in-service laminated glass structures: Analytical, experimental and numerical investigations on delaminated beams. *Applied Sciences (Switzerland)*, *9*(18). https://doi.org/10.3390/app9183928

Butchart, C., & Overend, M. (2013). Influence of Moisture on the Post-fracture Performance of Laminated Glass. *Glass Performance Days 2013*.

Centelles, X., Martín, M., Solé, A., Castro, J. R., & Cabeza, L. F. (2020). Tensile test on interlayer materials for laminated glass under diverse ageing conditions and strain rates. *Construction and Building Materials*, *243*. https://doi.org/10.1016/j.conbuildmat.2020.118230

Chen, S., Chen, X., & Wu, X. (2018). The mechanical behaviour of polyvinyl butyral at intermediate strain rates and different temperatures. *Construction and Building Materials*, *182*. https://doi.org/10.1016/j.conbuildmat.2018.06.080

Delincé, D., Belis, J., Zarmati, G., & Parmentier, B. (2007). Structural behaviour of laminated glass elements – a step towards standardization. *Glass Performance Days 2007*.

Ensslen, F. (2007). Tragverhalten von Bewitterten Verbund-Sicherheitsglas-Scheiben. *Stahlbau*, *76*(8). https://doi.org/10.1002/stab.200710061

International Organization for Standardization. (2011). *Glass in building - Laminated glass and laminated safety glass - Part 4: Test methods for durability*. *European Committee for Normalization* (EN ISO 12543-4).

International Organization for Standardization. (2008). *Plastics-Determination of water absorption* (EN ISO 62).

ISC Security Design Criteria for New Federal Office Buildings and Major Modernization Projects. (2003). In *ISC Security Design Criteria for New Federal Office Buildings and Major Modernization Projects*. https://doi.org/10.17226/10678

Knight, J. (2020). "Experimental Evaluation of Laminated Glass Interlayer Polymers at Various Strain Rates and Temperatures." University of Missouri.

Martín, M., Centelles, X., Solé, A., Barreneche, C., Fernández, A. I., & Cabeza, L. F. (2020). Polymeric interlayer materials for laminated glass: A review. In *Construction and Building Materials* (Vol. 230). https://doi.org/10.1016/j.conbuildmat.2019.116897

Nawar, M. (2016). "Numerical modeling and experimental evaluation of laminated glazing systems and material under blast loading." University of Missouri.

Ranocchiai, G., Andreozzi, L., Zulli, F., & Fagone, M. (2016). Effects of interlayer weathering on the structural behaviour of laminated glass structures. *Challenging Glass Conference Proceedings - Challenging Glass 5: Conference on Architectural and Structural Applications of Glass, CGC 2016*.

Saad, G. R., El-Shafee, E., & Sabaa, M. W. (1995). Dielectric and mechanical properties in the photodegradation of poly(vinyl butyral) films. *Polymer Degradation and Stability*, *47*(2). https://doi.org/10.1016/0141-3910(94)00111-K

Serafinavicius, T., Lebet, J. P., Louter, C., Kuranovas, A., & Lenkimas, T. (2014). The effects of environmental impacts on durability of laminated glass plates with interlayers (SG, EVA, PVB). *Challenging Glass 4 and COST Action TU0905 Final Conference - Proceedings of the Challenging Glass 4 and Cost Action TU0905 Final Conference*. https://doi.org/10.1201/b16499-66

Teotia, M., & Soni, R. K. (2014). Polymer Interlayers for Glass Lamination - A Review. *International Journal of Science and Research*, *3*(8).

Weller, B., & Kothe, M. (2011). Ageing Behaviour of Polymeric Interlayer Materials and Laminates. *Glass Performance Days*.

Zhang, X., Hao, H., Shi, Y., & Cui, J. (2015). The mechanical properties of Polyvinyl Butyral (PVB) at high strain rates. *Construction and Building Materials*, *93*. https://doi.org/10.1016/j.conbuildmat.2015.04.057

7 APPENDIX-PHOTOTRACK

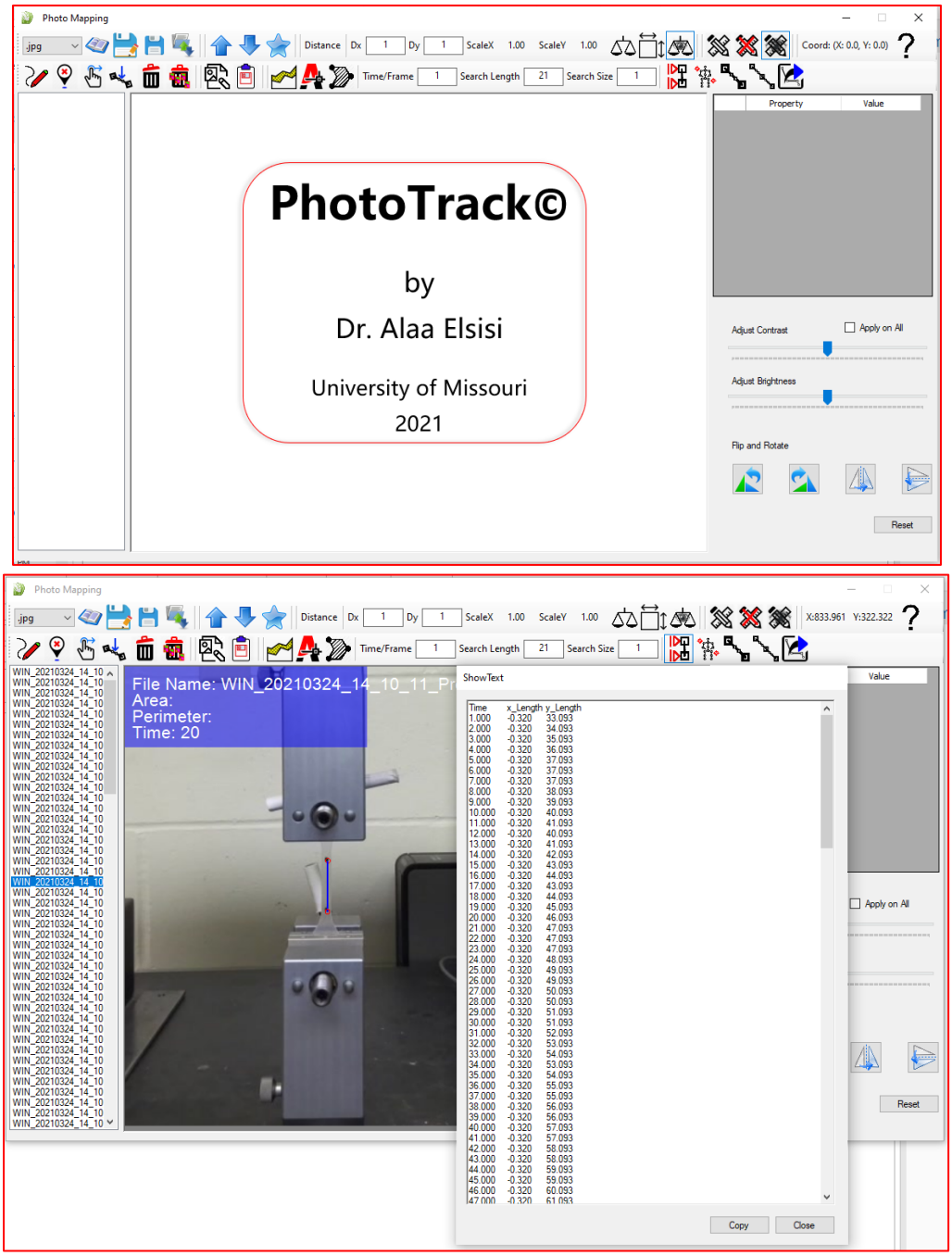

PhotoTrack Software Screenshots

7.1 PHOTOTRACK SOURCE CODE

```
using System;
using System.Collections.Generic;
using System.ComponentModel;
using System.Data;
using System.Drawing;
using System.Linq;
using System.Text;
using System.Windows.Forms;
using System.IO;
using SmartControl;
namespace PhotoTrack
{
   public partial class frmMain : Form
   {
      DatSet[] LST ;
      string[] filePaths;
      int x1 = -10;
      int x2 = -5;
      int x3 = -2;
      int y1 = -5;
      int y2 = -2;
      double F_Width = 0;
      double F_Height = 0;
      DatSet STemp;
      public frmMain()
      {
```

```
    InitializeComponent();
}

private void zoomPanPanel1_Click(object sender, EventArgs e)
{

}

private void vScrollBar1_Scroll(object sender, ScrollEventArgs e)
{
    //y1 = vScrollBar1.Value;
    //zoomPanPanel1.   DrawLines(x1, x2, x3, y1, y2);

}

private void vScrollBar2_Scroll(object sender, ScrollEventArgs e)
{
   // y2 = vScrollBar2.Value;
    zoomPanPanel1.DrawLines(x1, x2, x3, y1, y2);

}

private void hScrollBar1_Scroll(object sender, ScrollEventArgs e)
{
    /*
    x1 = hScrollBar1.Value;
    if (x2 <= x1)
```

```
    {
        x2 = x1 + 5;
        hScrollBar2.Value=x2;
    }
    if (x3 <= x2)
    {
        x3 = x2 + 5;
        hScrollBar3.Value=x3;
    }

    zoomPanPanel1.DrawLines(x1, x2, x3, y1, y2);
     * */
}
private void hScrollBar2_Scroll(object sender, ScrollEventArgs e)
{
     /*
    x2 = hScrollBar2.Value;
    if (x3 <= x2)
    {
        x3 = x2 + 5;
        hScrollBar3.Value = x3;
    }
    if (x2 <= x1)
    {
        x1 = x2 - 5;
        hScrollBar3.Value = x3;
    }
```

```
    zoomPanPanel1.DrawLines(x1, x2, x3, y1, y2);
     * */
}

private void hScrollBar3_Scroll(object sender, ScrollEventArgs e)
{
    /*
    x3 = hScrollBar3.Value;
    if (x3 <= x2)
    {
        x2 = x3 - 5;
        hScrollBar3.Value = x3;
    }
    zoomPanPanel1.DrawLines(x1, x2, x3, y1, y2);
     * */
}
private void ReadNext()
{
    int i=ImgList.SelectedIndex;
    if (i >= 0 && i + 1 < ImgList.Items.Count)
    {
        OpenImage(i+1);
        ImgList.SelectedIndex = i + 1;
    }
}
private void ReadPrevious()
{
```

```
    int i = ImgList.SelectedIndex;
    if (i-1 >= 0 && i < ImgList.Items.Count)
    {
        OpenImage(i-1);
        ImgList.SelectedIndex = i -1;
    }
}
private void Form1_MouseMove(object sender, MouseEventArgs e)
{
    //button1.Text = e.X.ToString();

}

private void Form1_Load(object sender, EventArgs e)
{
    Extens.Items.Add(".jpg");
    Extens.Items.Add(".tif");
    Extens.Items.Add(".tiff");
    Extens.Items.Add(".png");
    Extens.Items.Add(".bmp");
    Extens.SelectedIndex = 0;
    zoomPanPanel1.MyCoordinate = Coord;
    //this.Show();
    /*
    LicenseObtainer LicenseObtainerForm = new LicenseObtainer();
    LicenseObtainerForm.ShowDialog(this);
    if (LicenseObtainerForm.status == true)
```

```
        LicenseObtainerForm.Dispose();
    else
    {
        LicenseObtainerForm.Dispose();
        this.Dispose();
    }
     * */

}
protected override void OnMouseWheel(MouseEventArgs e)
{

}


private void button3_Click(object sender, EventArgs e)
{
    //zoomPanPanel1.
    folderBrowserDialog1.ShowDialog();
    string CurrentFolder = folderBrowserDialog1.SelectedPath;

}

private void zoomPanPanel1_Paint(object sender, PaintEventArgs e)
{

}
```

```
private void zoomPanPanel1_Paint_1(object sender, PaintEventArgs e)
{

}

private void OpenImage(int i)
{
   try
   {
      if (LST[i] != null)
      {
         STemp = LST[i];

      }
      else
      {
         STemp = new DatSet();
         STemp.IMG = i;
         LST[i] = STemp;
      }

      zoomPanPanel1.Marks = STemp;

      float zmm = zoomPanPanel1.Zoom;
      PointF pcntr = zoomPanPanel1.viewPortCenter;
      Bitmap BTM = new Bitmap(filePaths[i]);
```

```
            if (i == 0)
            {
               F_Height = BTM.Height;
               F_Width = BTM.Width;
            }


            //zoomPanPanel1.Width = BTM.Width;
            //zoomPanPanel1.Height = BTM.Height;
            zoomPanPanel1.Bitmap = null;
            zoomPanPanel1.Bitmap = BTM;
            zoomPanPanel1.Zoom = zmm;
            zoomPanPanel1.frst = true;
            if (pcntr.X != 0f && pcntr.Y != 0f)
               zoomPanPanel1.viewPortCenter = pcntr;
            //hScrollBar1.Maximum = BTM.Width;
            //hScrollBar2.Maximum = BTM.Width;
            //hScrollBar3.Maximum = BTM.Width;
            //vScrollBar1.Maximum = BTM.Height;
            //vScrollBar2.Maximum = BTM.Height;
            //hScrollBar1.Top = zoomPanPanel1.Bottom + 5;
            //hScrollBar2.Top = hScrollBar1.Bottom + 2;
            //hScrollBar3.Top = hScrollBar2.Bottom + 2;
            //this.Height = zoomPanPanel1.Height + hScrollBar1.Height +
hScrollBar2.Height + hScrollBar3.Height + 120;
            //pictureBox2.Height = zoomPanPanel1.Height;
```

```
        //pictureBox2.Left = zoomPanPanel1.Right;
        //vScrollBar1.Height = zoomPanPanel1.Height;
        //vScrollBar2.Height = zoomPanPanel1.Height;
        ImgList.SelectedIndex = i;

    }


    catch(Exception e)

    {


    }



}

private void CmdOpen_Click(object sender, EventArgs e)
{

    if (    FolderTool.ShowDialog()== DialogResult.OK)
    {
        ImgList.Items.Clear();
        filePaths = null;
```

```
        filePaths = Directory.GetFiles(FolderTool.SelectedPath, "*"+Extens.Text);

        for (int i = 0; i < filePaths.Length; i++)
        {
            string[] s = filePaths[i].Split('\\');
            ImgList.Items.Add(s[s.Length-1]);
        }
         LST = new DatSet[filePaths.Length];

        OpenImage(0);
    }
}

private void button4_Click(object sender, EventArgs e)
{

}
private void CmdAnalyze_Click(object sender, EventArgs e)
{
    int m = 0;
    if (LST == null)
    {
        MessageBox.Show("Please Check Your Inputs");
        return;
    }

    try
```

```
    {
        for ( m = 0; m < LST.Length - 1; m++)
        {

            //if (m == 90)
            //{
                //MessageBox.Show("Please Check Your Inputs");

            //}



            PointF P1 = LST[m].P1;
            LST[m + 1] = new DatSet();
            LST[m + 1].P1 = Track( m,  P1);
            PointF P2 = LST[m].P2;
            LST[m + 1].P2 = Track(m, P2);

            ImgList.SelectedIndex = m;
        }
    }
    catch (Exception e1)
    {


    }
}
```

```
    private void toolStrip1_ItemClicked(object sender, ToolStripItemClickedEventArgs
e)
    {

    }

    private void CmdPrev_Click(object sender, EventArgs e)
    {
       ReadPrevious();
    }

    private void CmdNext_Click(object sender, EventArgs e)
    {
       ReadNext();
    }

    private void ImgList_SelectedIndexChanged(object sender, EventArgs e)
    {
       OpenImage(ImgList.SelectedIndex);
    }

    private void CmdCollect_Click(object sender, EventArgs e)
    {
       zoomPanPanel1.Collect();
    }
```

```
        private void toolStrip1_ItemClicked()
        {


        }


        private void CmdExtract_Click(object sender, EventArgs e)
        {
            if (LST == null)
            {
                MessageBox.Show("Please Check Your Inputs");
                return;
            }
            double T = 0;
            SaveFileDialog saveFileDialog = new SaveFileDialog();
            saveFileDialog.InitialDirectory =
Environment.GetFolderPath(Environment.SpecialFolder.Personal);
            saveFileDialog.Filter = "Data Files (*.txt)|*.txt|All Files (*.*)|*.*";
            if (saveFileDialog.ShowDialog(this) == DialogResult.OK)
            {
                string FileName = saveFileDialog.FileName;
                string line;
                // Read the file and display it line by line.
                using (StreamWriter writer = File.CreateText(FileName))
                {
                    line = "Time" + "\t" + "x_Length" + "\t" + "y_Length" + "\t" + "x_Velocity"
+ "\t" + "y_Velocity"
    + "\t" + "x_Accel" + "\t" + "y_Accel";
                    writer.WriteLine(line);
```

```
            double Lx1 = (LST[0].P2.X -
LST[0].P1.X)/F_Width*TxtWidth.DoubleValue;

            double Ly1 = (LST[0].P2.Y - LST[0].P1.Y) / F_Height *
((NumericTextBox)this.TxtHeight).DoubleValue;

            double Vx1 = 0;

            double Vy1 = 0;

            for (int m = 1; m < LST.Length; m++)

            {

               double Lx2 = (LST[m].P2.X - LST[m].P1.X) / F_Width *
TxtWidth.DoubleValue;

               double Ly2 = (LST[m].P2.Y - LST[m].P1.Y) / F_Height *
((NumericTextBox)this.TxtHeight).DoubleValue;

               T =T+ txtdT.DoubleValue;

               double Vx2 = Lx2 / txtdT.DoubleValue;

               double Vy2 = Ly2 / txtdT.DoubleValue;


               double ax = (Vx2 - Vx1) / txtdT.DoubleValue;

               double ay = (Vy2 - Vy1) / txtdT.DoubleValue;




               line = T.ToString("F3") + "\t" + Lx2.ToString("F3") + "\t" +
Ly2.ToString("F3") + "\t" + Vx2.ToString("F3") + "\t" + Vy2.ToString("F3")
                    + "\t" + ax.ToString("F3") + "\t" + ay.ToString("F3");

               writer.WriteLine(line);

               Lx1 = Lx2;

               Ly1 = Ly2;

               Vx1 = Vx2;

               Vy1 = Vx2;
```

```
            }

        }

    }
}

    private void toolStripButton1_Click(object sender, EventArgs e)
    {
        AboutBox1 ABT = new AboutBox1();
        ABT.ShowDialog(this);

    }
  }
}
```